Article

Exploring the Utility of ssDNA Aptamers Directed against Snake Venom Toxins as New Therapeutics for Snakebite Envenoming

Nessrin Alomran [1], Raja Chinnappan [2,3] , Jaffer Alsolaiss [1] , Nicholas R. Casewell [1,4,]* and Mohammed Zourob [2,3,]*

1. Centre for Snakebite Research & Interventions, Liverpool School of Tropical Medicine, Pembroke Place, Liverpool L3 5QA, UK; nessrin.alomran@lstmed.ac.uk (N.A.); jaffer.alsolaiss@lstmed.ac.uk (J.A.)
2. Department of Chemistry, Alfaisal University, Al Zahrawi Street, Al Maather, Al Takhassusi Road, Riyadh 11533, Saudi Arabia; rchinnappan@alfaisal.edu
3. King Faisal Specialist Hospital and Research Center, Zahrawi Street, Al Maather, Riyadh 12713, Saudi Arabia
4. Centre for Drugs and Diagnostics, Liverpool School of Tropical Medicine, Pembroke Place, Liverpool L3 5QA, UK
* Correspondence: nicholas.casewell@lstmed.ac.uk (N.R.C.); mzourob@alfaisal.edu (M.Z.)

Abstract: Snakebite is a neglected tropical disease that causes considerable death and disability in the tropical world. Although snakebite can cause a variety of pathologies in victims, haemotoxic effects are particularly common and are typically characterised by haemorrhage and/or venom-induced consumption coagulopathy. Antivenoms are the mainstay therapy for treating the toxic effects of snakebite, but despite saving thousands of lives annually, these therapies are associated with limited cross-snake species efficacy due to venom variation, which ultimately restricts their therapeutic utility to particular geographical regions. In this study, we sought to explore the potential of ssDNA aptamers as toxin-specific inhibitory alternatives to antibodies. As a proof of principle model, we selected snake venom serine protease toxins, which are responsible for contributing to venom-induced coagulopathy following snakebite envenoming, as our target. Using SELEX technology, we selected ssDNA aptamers against recombinantly expressed versions of the fibrinogenolytic SVSPs ancrod from the venom of *C. rhodostoma* and batroxobin from *B. atrox*. From the resulting pool of specific ssDNA aptamers directed against each target, we identified candidates that exhibited low nanomolar binding affinities to their targets. Downstream aptamer-linked immobilised sorbent assay, fibrinogenolysis, and coagulation profiling experiments demonstrated that the candidate aptamers were able to recognise native and recombinant SVSP toxins and inhibit the toxin- and venom-induced prolongation of plasma clotting times and the consumption of fibrinogen, with inhibitory potencies highly comparable to commercial polyvalent antivenoms. Our findings demonstrate that rationally selected toxin-specific aptamers can exhibit broad in vitro cross-reactivity against toxin isoforms found in different snake venoms and are capable of inhibiting toxins in pathologically relevant in vitro and ex vivo models of venom activity. These data highlight the potential utility of ssDNA aptamers as novel toxin-inhibiting therapeutics of value for tackling snakebite envenoming.

Keywords: snakebite envenoming; snake venom serine proteases; recombinant toxins; SELEX selection; in vitro assays; ssDNA aptamers

Key Contribution: This paper demonstrates that ssDNA aptamers directed against recombinant snake venom toxins exhibit promising in vitro binding and inhibitory capabilities and advocates for further research to assess the potential utility of aptamers as novel snakebite therapeutics.

1. Introduction

Snakebite envenoming is a significant public health issue as more than 5.4 million people are bitten annually by venomous snakes, and this mainly affects resource-poor

communities in the rural tropics and subtropics across Africa, the Americas, Asia, the Middle East, and Australasia [1–3]. Since 2017, snakebite has been classified by the World Health Organization as a neglected tropical disease [4]. Snake venom is a potentially lethal and complex mixture of hundreds of functional toxins that vary extensively among snake species [5,6]. Despite such variation, the various toxins present can be broadly classified into three major categories of pathology that they cause in snakebite victims: haemotoxicity, neurotoxicity and cytotoxicity [7].

Envenomings by viperid snakes (Viperinae, true vipers; Crotalinae, pit vipers) are predominately responsible for causing haemotoxicity and are systemically characterised by causing overt haemorrhage, such as from the gums, and internal haemorrhage, such as intracranially [7,8]. Snakebite-induced coagulopathy, i.e., defibrinogenation, also known as venom-induced consumption coagulopathy (VICC), is one of the most common life-threatening and important systemic pathologies observed following snakebite [2,9–11]. VICC is caused by the bites of a wide range of snakes, including many true vipers and pit vipers (e.g., *Daboia russelii*, *Calloselasma rhodostoma*, etc.), certain Australasian elapids (e.g., *Oxyuranus scutellatus*) and a few colubrid snakes (e.g., *Dispholidus typus*) [12,13].

The venom toxins primarily thought to be responsible for causing VICC are members of the snake venom metalloproteinase (SVMP) and snake venom serine protease (SVSP) toxin families [14,15]. Each of these toxin families is multi-locus in nature, with related genes producing the multiple protein isoforms found in venom which, as the result of protein neofunctionalisation, typically exhibit distinct functional activities [7,13,16]. Snakebite coagulopathy disorders result from the consumption of clotting factors (e.g., Factor X, V and prothrombin) [15] via initial toxin-induced cleavage stimulating the activation of the coagulation cascade, resulting in the abnormal and continual activation of downstream clotting factors, and a loss of clotting capability via depletion of fibrinogen [13,16]. However, some toxins also act directly on fibrinogen in a fibrinogenolytic manner [15], and many venoms contain both upstream clotting factor activators and fibrinogenolytic toxins simultaneously. Thus, venom toxins can result in hypofibrinogenaemia, with either no formation of fibrin due to the cleavage of the fibrinogen α-chain and/or β-chain by thrombin-like enzymes or fibrinogenases (typically SVSP toxins), or afibrinogenaemia (the absence of circulating fibrinogen) due to depletion via upstream coagulation cascade activation [17]. While this combination of procoagulant and anticoagulant toxins present in snake venom [18] can rapidly lead to a loss of clotting capability in envenomed victims [9,15,17], the severity of envenoming can be further exacerbated by other toxins (e.g., SVMPs) simultaneously stimulating widespread haemorrhage by disrupting the integrity of the microvasculature via cleavage of extracellular matrix proteins [19,20].

Antivenoms, which consist of animal-derived polyclonal antibodies derived from hyperimmunised serum/plasma, remain the only specific therapeutic to combat the toxicity of snakebite envenoming [21]. Although antivenoms are life-saving therapeutics, they are also associated with several limitations that affect their efficacy, safety, and utility in the tropical world. For example, the intravenous delivery of animal-derived antibodies comes with an associated risk of adverse reactions, which may include vomiting, urticaria, generalised rash or, in rarer cases, more severe effects (e.g., anaphylactic shock) [22–25]. In addition, only 10–20% of antivenom antibodies are typically specific to the venom immunogens [26] as venom-immunised animals are exposed to other environmental stimuli and toxin-specificity is typically not selected for from the resulting antibody pool. Perhaps most importantly, antivenoms exhibit limited cross-snake species efficacy as the direct result of variation in venom composition among medically important snake species [6,27]. Thus, antivenom efficacy is largely restricted to the snake species or those closely-related to or with similar venom compositions to those used during the immunisation process [28]. The result of limited paraspecific antivenom efficacy is a fragmented drug market, with numerous antivenoms manufactured around the world with specificity against certain snake species and, thus, restricted for use in specific geographical regions. Antivenoms are also often unaffordable to patients, as treatment courses frequently necessitate the administration

of multiple vials (ranging from 3 to 30 vials depending on region and product), resulting in costs exceeding USD 1000 in parts of sub-Saharan Africa, for example [29]. This cost pushes many tropical snakebite victims further into poverty [30,31].

In response to the above, recent research has focused on applying alternate therapeutic strategies to circumvent the limitations currently associated with conventional antivenoms. Promising approaches explored to date include the use of toxin-specific monoclonal antibodies [32], small-molecule drugs [33], decoy receptor binding proteins [34] and aptamers [35–37]. Although arguably the least studied of these approaches in the context of snakebite, single-stranded DNA (ssDNA) aptamers have emerged as promising alternatives to antibodies in various biosensing platforms and as the biological recognition element for therapeutic applications and diagnostic tools for different diseases [38–40]. Aptamers are short ssDNA (or ssRNA) molecules that can bind to their target and fold into complex and stable three-dimensional shapes [41,42] with high specificity and affinity through hydrogen bonding, van der Waals forces, hydrophobic, salt bridges and other electrostatic interactions [43–46]. Consequently, aptamers act like antibodies by binding and inhibiting target antigens and, thus, have been referred to as chemical antibodies due to their synthetic production [47,48]. ssDNA aptamers possess several advantages over antibodies as, in addition to seemingly exhibiting comparable high-affinity recognition properties (i.e., dissociation constants in the low nanomolar (nM)/picomolar (pM) range) [43,44,49], they are highly specific, sensitive, and chemically stable with long shelf lives [50–52] and require facile artificial synthesis [53], resulting in high purity, low interbatch variability and cost-effective production [54–56]. Further, ssDNA aptamers are poorly immunogenic, which aids their tolerance, and due to their small size, they diffuse readily into tissues [57]. However, this latter characteristic also causes challenges, as the in vivo half-life of ssDNA aptamers is much shorter (~20 min) than antibodies (e.g., potentially a few days to weeks) [58], though prolonged circulation can be improved by chemical modification [57,59–61]. Despite the therapeutic promise of aptamers, to date, the only FDA-approved aptamer remains the macular degeneration treatment Macugen® (Pegaptanib), which was first licensed in 2005 [62]. Since then, no other aptamers have entered the market, although many candidate aptamers have entered clinical trials over the past decade as promising new treatments for heart disease, cancer and type II diabetes [62].

ssDNA aptamers are typically selected by Systematic Evolution of Ligands by Exponential enrichment (SELEX) technology, which was introduced by Ellington and Tuerk three decades ago [43,44]. This process is based on the isolation of high-affinity ligands from a combinatorial ssDNA library (approximately 10^{17} random sequence oligonucleotides) through repeated cycles (usually requiring seven to fifteen rounds) of binding, elution, and amplification to select for oligonucleotides with the desired specificity and/or sensitivity [48,63,64]. Following cyclical SELEX enrichment, the final ssDNA aptamer pool is subjected to sequencing to identify the optimal resulting binding sequences, which are then manufactured by chemical synthesis and downstream-optimized by the introduction of chemical modifications to further improve their pharmacokinetic and/or pharmacodynamic profiles [65]. To date, several ssDNA aptamers have been successfully selected for and applied against a wide range of targets that include proteins, peptides, small organic compounds, carbohydrates, metal ions and biological cofactors [66–72]. In addition, ssDNA aptamers have been shown to bind to highly toxic native antigens, which, due to toxicity, cannot be achieved in animal-based methods to generate specific antibodies without antigen modification [73]. In the context of animal toxins, little work has been done, though aptamers have been selected against the three-finger toxin α-bungarotoxin from *Bungarus multicinctus* venom [74] and shown to exhibit cross-recognition and inhibitory activity against cytotoxins from *Naja atra* venom, which share similar tertiary structures [37]. Another recent study selected ssDNA aptamers against Indian *Bungarus caeruleus* venom and used them in a diagnostic context to discriminate envenomings by this species from those of other medically important snakes found in the region [75].

In this study, we sought to explore the potential utility of ssDNA aptamers against snake venom SVSP toxins responsible for contributing to venom-induced coagulopathy following snakebite envenoming. Using SELEX technology, we selected ssDNA aptamers against recombinantly expressed versions of the fibrinogenolytic SVSPs ancrod from the venom of *C. rhodostoma* and batroxobin from *Bothrops atrox*. Downstream ssDNA aptamer-linked immobilised sorbent assay (ALISA), fibrinogenolysis, and coagulation experiments demonstrated that the rationally selected ssDNA aptamers were able to recognise native and recombinant SVSP toxins and inhibit the toxin- and venom-induced prolongation of plasma clotting times and the consumption of fibrinogen. These data highlight the potential utility of ssDNA aptamers as novel toxin-inhibiting therapeutics and alternative binding scaffolds for future treatment strategies targeting tropical snakebites.

2. Results

2.1. ssDNA Aptamer Selection

Here, we report the identification of ssDNA aptamers that target the recombinantly expressed SVSP toxins ancrod from *C. rhodostoma* and batroxobin from *B. atrox*, which we previously expressed in human embryonic kidney mammalian cell lines (HEK293) [76]. To do so, we employed a parallel process consisting of 14 rounds of SELEX selections against each toxin target using an ssDNA library pool of 10^{17} random sequences. The selection process was monitored throughout by polymerase chain reaction (PCR) amplification of the eluted double-stranded DNA (dsDNA) and visualised by using 2% agarose gel electrophoresis (Figure 1A,B) and by measuring the fluorescence intensity of the eluted ssDNA solution by using denaturing polyacrylamide gel electrophoresis (PAGE) (Figure 1C,D).

Our findings revealed that initial DNA recovery against each target was low, though this increased with progressive rounds of selection cycles until a marked increase was observed at round 11, indicating enrichment of the DNA pool with sequences specific to the toxins coupled to the beads (Figure 1). Notably, the patterns of fluorescent intensities obtained from the sequential selection rounds were highly comparable between the two toxin targets (Figure 1). Counter-selection (CS) was performed at round 12 to eliminate non-specific ssDNA interacting with the Sepharose beads instead of the toxins, and this resulted in an anticipated drop in the fluorescence intensity of the recovered DNA (Figure 1C,D). Thereafter, two additional rounds of SELEX selection were performed to secondarily enrich toxin-specific aptamers, which resulted in an increase in fluorescence intensity at round 13 but no further increase at round 14, suggesting that target binding sites might be saturated (Figure 1C,D). Consequently, SELEX selection was stopped, and the resulting ssDNA from the last round (round 14) was cloned for downstream aptamer identification.

Cloning was performed by ligation into a cloning vector and transformation into *E. coli* competent cells, with validation performed on ten random colonies to demonstrate that the inserted DNA (300 bp) was successfully ligated into the pCR2.1-TOPO cloning vector (3956 bp) (Figure 1E,F). Thereafter, 100 colonies were picked for each toxin target and subjected to PCR, followed by Sanger sequencing. Bioinformatic analyses of the resulting DNA identified various identical sequences, indicating enrichment of the DNA pool, and resulted in thirteen and nine unique aptamer sequences against ancrod and batroxobin, respectively (Table 1).
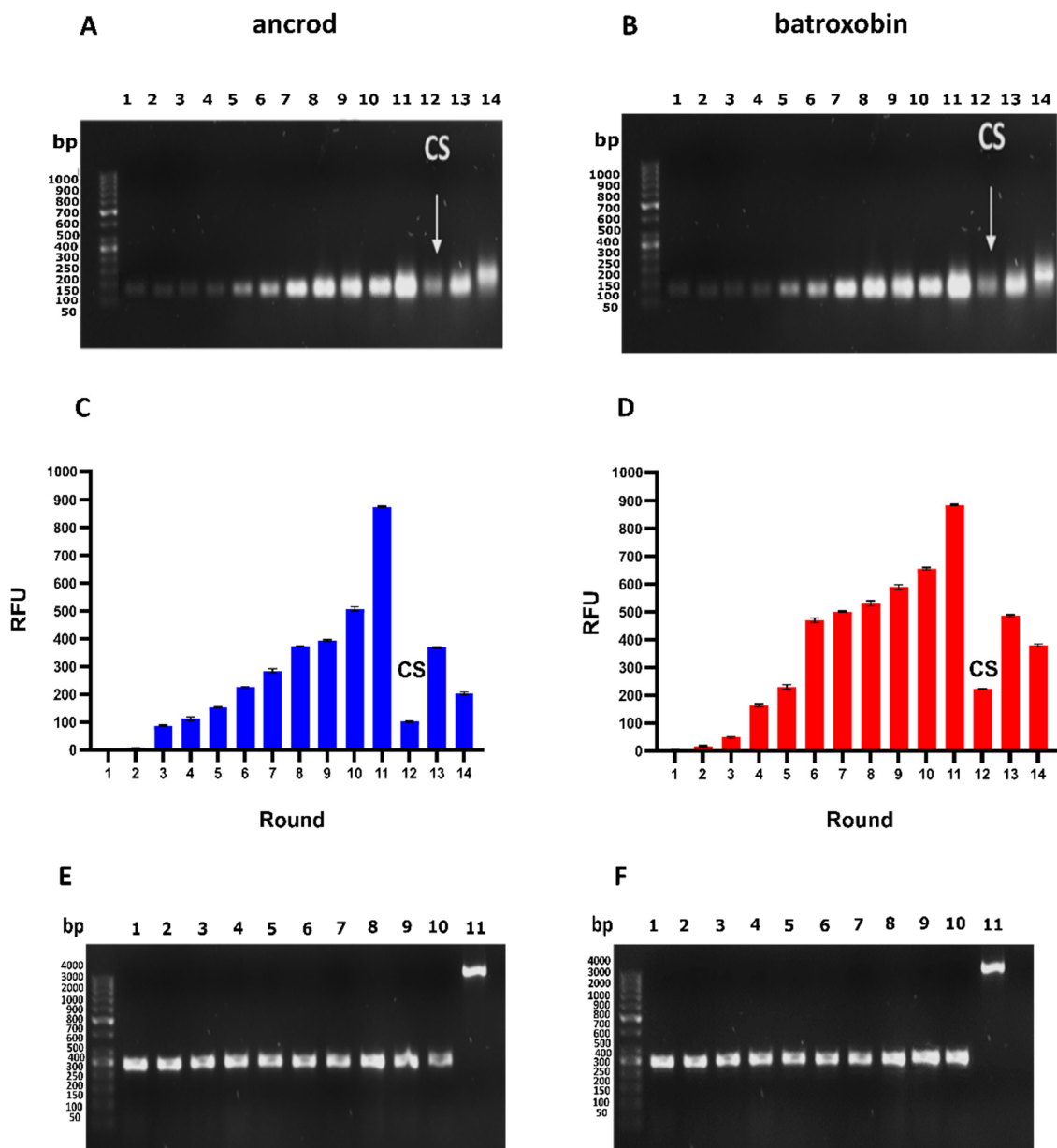
Figure 1. Sequential SELEX selection of aptamers against the recombinant SVSP toxins ancrod and batroxobin. (**A**,**B**) DNA was amplified by PCR for each round of toxin selection employed (Lane 1–14; size, DNA $\approx$ 104 bp), with non-specific bound ssDNA eliminated by counter-selection (CS, highlighted by arrow) employed at round 12. Data for ancrod are shown in (**A**) and batroxobin in (**B**). (**C**,**D**) The fluorescence intensity of the eluted ssDNA solution from each round of selection was measured at an excitation wavelength of 470 nm and an emission of 515 nm. Error bars represent the standard error (SEM) of triplicate measurements, with data for ancrod shown in (**C**) and batroxobin in (**D**). (**E**,**F**) Colony PCR was performed by ligation into a cloning vector and transformation into E. coli competent cells, with validation performed on ten random colonies to demonstrate that the inserted DNA (Lane 1–10; size $\approx$ 300 bp) was successfully ligated into the pCR2.1-TOPO cloning vector (Lane 11; size $\approx$ 3956 bp). Data for ancrod are shown in (**E**) and batroxobin in (**F**).

Table 1. The identity of the unique ssDNA aptamers selected against ancrod and batroxobin.

Target	Aptamer Identifier	The Sequence of the Random Region (5′-3′)
ancrod	ancrod-1	TGCTCACACGTCCTGTGTGATTATGTCAGGCATTCACATG
	ancrod-2	TGCTGGGAAATCCTCCCATTATGTCAGTATGTCTCGACAT
	ancrod-5	ACGCTTGATCCTCCGAAATGTCCTGATCCTCGGCCTGTCA
	ancrod-7	TAGCATGGGTGGTCAATTTAAGTACAGTGTCGTGCTCACT
	ancrod-11	TGGTCTAAGGACTGCTTAGGATTGCGATATGGTCCAGATG
	ancrod-12	GTAAATTGTACAGGTGTATGGATTGCTAGGTCTGCTGGTT
	ancrod-18	TGTCTGGTTTGCAAAGGACTGCTGTACTGTTAGCTTTTGT
	ancrod-25	GGTGCGTTTCACCTCGAGTTTACGATAAATCACCTTCGAG
	ancrod-30	TATTAAGGGACTGCTCGGGATTGCGGATATAGGTATGAGC
	ancrod-31	GTGTATTGTGATAGTCGGTAATTCCCTGACTACGCCGTAT
	ancrod-32	TTGGGCCCTCTAGTGATGGATATCTGCAGAATTCGCCCTT
	ncrod-48	TAGTAACAGGTCTGCTTAGGCTTGCGAGGAATACTAGTAC
	ancrod-55	GGACCGACCCTTTAGCATTTATGACCCTTGTCATCGGGCT
batroxobin	batroxobin-4	AGGTGGTCAGCTTTATCCTTTATGACCTTAACCCGTCATG
	batroxobin-5	TAGTAACAGGTCTGCTTAGGCTTGCGAGGAGTACTAGTAT
	batroxobin-6	AGGTGGATATCAAGATAGGTTTGGTTAGGTAGCGTTCTTG
	batroxobin-14	GGACCGACCCTTTAGCATTTATGACCCTTGTCATCGGGCT
	batroxobin-18	TGCTGGGAAATCCTCCCATTATGTCAGTATGTCTCAACAT
	batroxobin-21	AGGGGGCGACCTTTAATGCTTGTGATCCTTATCCGTCATC
	batroxobin-26	TGTCTGGTATGCAAAGGACTGCTGTACTGTTAGCTTTTGT
	batroxobin-28	TAGCATGGGTGGTCAATTTAAGTACAGTGTCGTGCTCACT
	batroxobin-29	AGGTCCTATTGTATACAGGGAGCCCTCGGTCTTGCTGTGA

2.2. Dissociation Constants of Identified Aptamers

The dissociation constants (K_d) for each of the selected ssDNA aptamers were determined via the nonlinear regression of saturation graphs resulting from concentration-based fluorescence binding assays. Of the 22 aptamers tested, only three ssDNA aptamer sequences directed against each of the targets exhibited nanomolar affinity, with those targeting ancrod ranging from 3.0 to 17.8 nM and those against batroxobin ranging from 4.7 to 24.3 nM (Figure 2). The remaining ssDNA aptamers exhibited high K_d readings and were excluded from further study. The candidate ssDNA aptamer sequences with the lowest K_d were ancrod-55 (K_d = 3.0 nM) and batroxobin-26 (K_d = 4.7 nM) (Figure 2); thus, these two aptamers were selected for downstream recombinant toxin/crude venom binding and inhibition experiments.
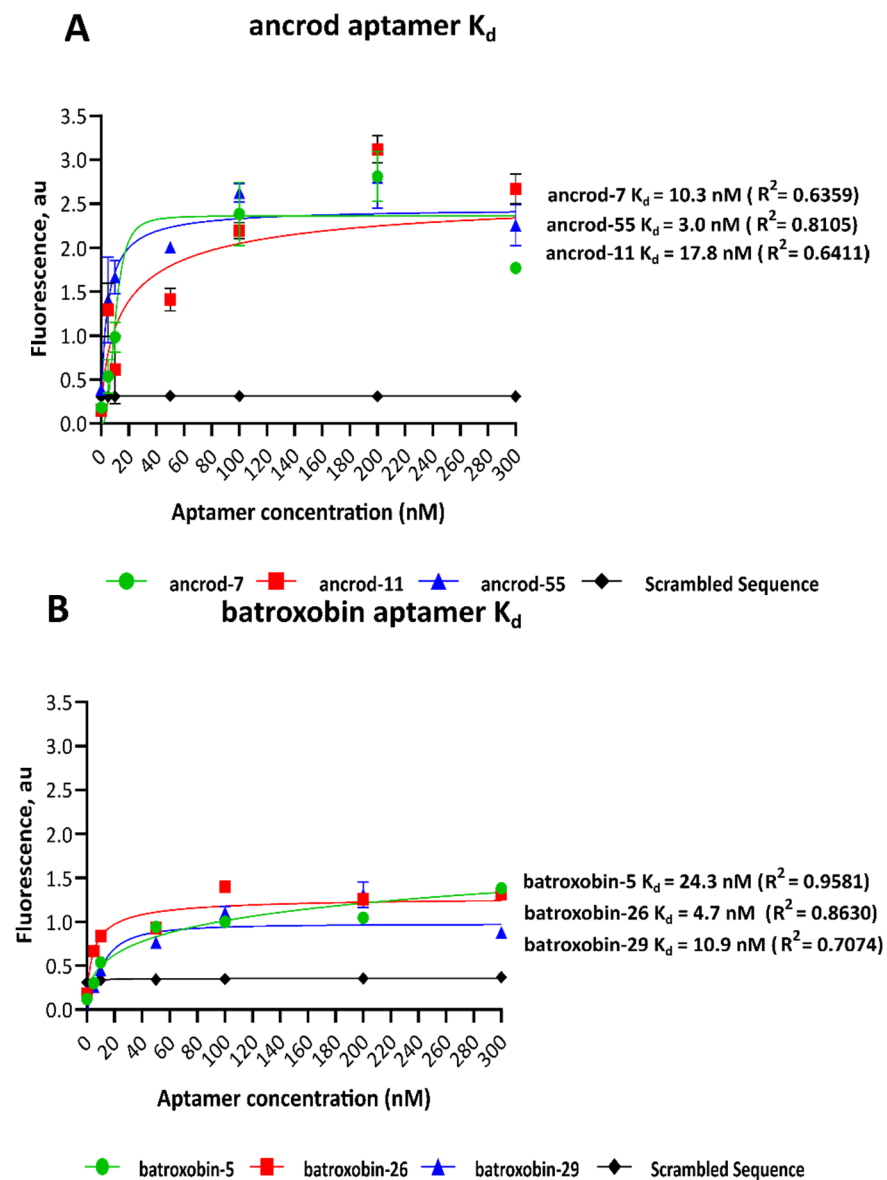
Figure 2. The equilibrium K_ds of the highest affinity ssDNA aptamers were derived from the fluorescence binding curves for each toxin target. The data shown represent the highest affinity candidate aptamers for ancrod (ancrod-7, ancrod-11 and ancrod-55) (**A**) and batroxobin (batroxobin-5, batroxobin-26 and batroxobin-29) (**B**). Concentration-dependent data were generated at an excitation wavelength of 470 nm and an emission of 515 nm, and K_ds were calculated via nonlinear regression analysis of the resulting saturation curves. Data represent means of duplicate measurements, and error bars represent standard deviations (SD).

2.3. Quantifying Aptamer Binding to Recombinant Toxins and Venom by ALISA

An ALISA was next used to quantify the binding levels of the two highest affinity aptamers (ancrod-55 and batroxobin-26) against each of the recombinant toxins and the native venoms from which the recombinant toxins were derived (i.e., *C. rhodostoma* and *B. atrox* venoms) in a reciprocal and comparative manner. The results of these binding assays, which were performed at two aptamer concentrations (0.4 and 2 nM), revealed that the two aptamers tested exhibited considerable cross-recognition and binding to the two SVSP toxins (i.e., irrespective of which toxin the aptamer was selected against) and the two homologous venoms (Figure 3). Indeed, the aptamer batroxobin-26 exhibited highly comparable binding levels to batroxobin, ancrod and the two native snake venoms

(Figure 3B). These binding levels were, however, lower than those obtained with the ancrod-55 aptamer for all comparisons (Figure 3A).
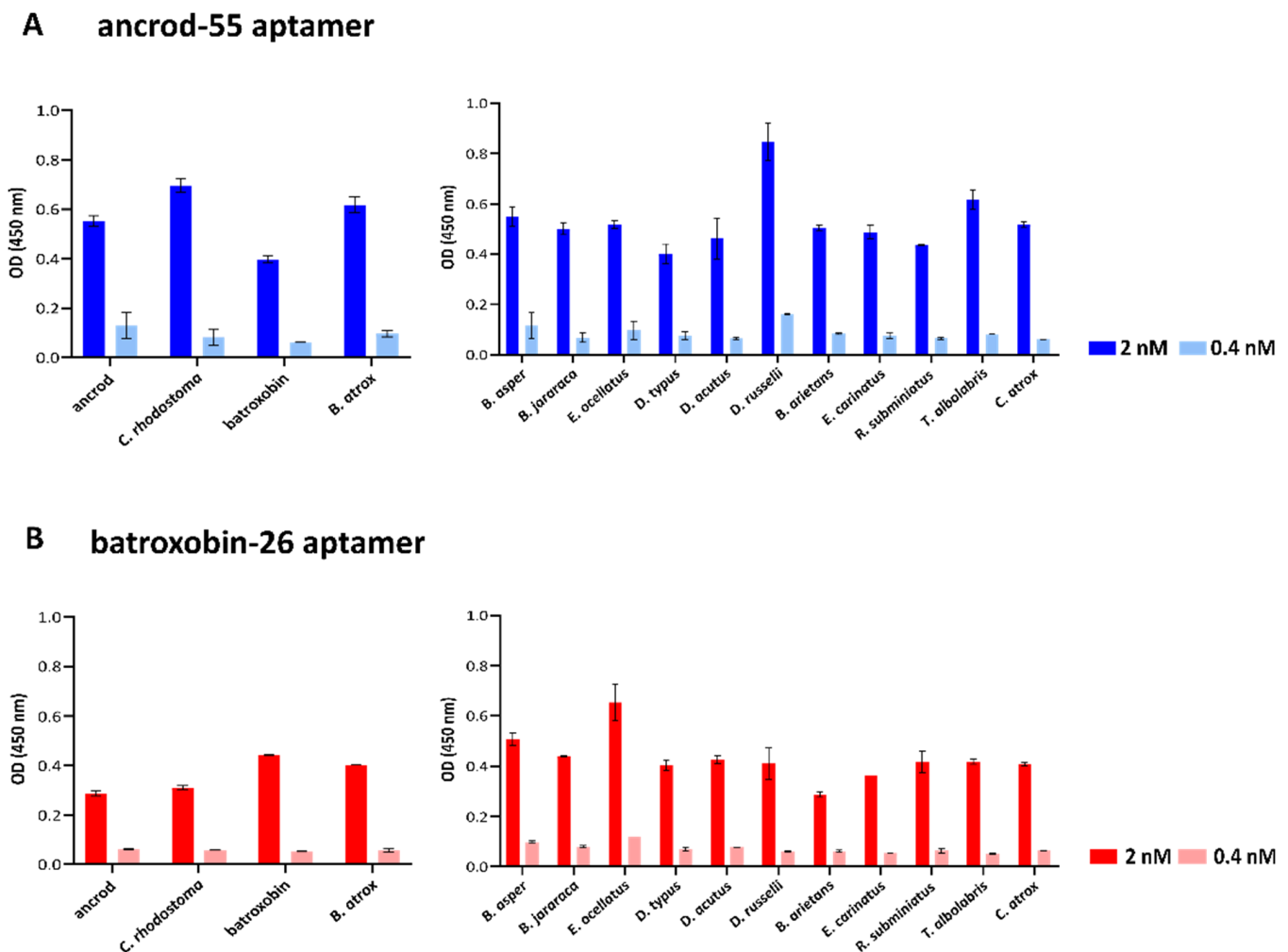

Figure 3. Quantification of binding levels between the selected ssDNA aptamers (ancrod-55 and batroxobin-26) and the SVSP recombinant toxins (ancrod and batroxobin) and a panel of native snake venoms by ALISA. Data are shown for the aptamers ancrod-55 (**A**) and batroxobin-26 (**B**). The data on the left show the binding levels obtained against the two recombinant toxins that the aptamers were selected against and the corresponding snake venoms that these toxins are derived from. The data on the right show binding levels obtained against a broad panel of 11 distinct snake venoms. All data represent the mean of duplicates measured at 450 nm, and error bars represent the standard deviation (SD) of the duplicate measurements.

Next, ALISA was used to explore the capability of each aptamer to bind to a panel of 11 distinct venoms that exhibited considerable variation in toxin composition and were sourced from taxonomically diverse snake species [77]. The binding patterns obtained from these experiments suggest that the two aptamers, each selected against a single SVSP toxin, recognise distinct snake venoms to a similar extent as the toxins and homologous snake venoms described above. Thus, at the 2 nM concentration tested, the aptamer ancrod-55 exhibited a mean optical density (OD) (450 nm) of 0.53 nm (range 0.40–0.84 nm) against the 11 venoms, compared with 0.55 and 0.40 nm against ancrod and batroxobin and 0.70 and 0.62 nm against *C. rhodostoma* and *B. atrox* venoms, respectively (Figure 3A). Similarly, batroxobin-26 exhibited a mean OD of 0.43 nm (range 0.29–0.65 nm) against the various venoms, compared with 0.29 and 0.44 nm against ancrod and batroxobin and 0.31 and 0.40 nm against *C. rhodostoma* and *B. atrox* venoms, respectively (Figure 3B). While the

range in binding levels observed suggests a considerable degree of variation in terms of venom recognition, it is possible that this might simply reflect the relative abundance of SVSP toxins present in these different venoms.

2.4. Aptamers Inhibit Toxin-Induced Fibrinogenolysis and Fibrinogen Depletion

Many SVSP toxins exert a functional activity akin to thrombin by cleaving the α- or/and β-chains of fibrinogen, typically resulting in the release of fibrinopeptides rather than fibrin and, thus, ultimately contributing to dysregulation of coagulation via depletion of fibrinogen [78,79]. To assess whether the binding exhibited by the highest affinity ssDNA aptamers was capable of inhibiting the functional activities known from SVSPs, we first used SDS-PAGE to visualise aptamer-mediated protection against fibrinogenolysis. Our findings revealed that, in line with the known functional activities of native ancrod and batroxobin in recent work [76], both recombinantly expressed toxins cleaved the α-chain of fibrinogen (Figure 4A,B). We then assessed the inhibitory capability of the two candidate ssDNA aptamers to prevent this functional activity. Both ancrod-55 and batroxobin-26 aptamers protected against fibrinogenolysis caused by the corresponding recombinant toxin, resulting in the visualisation of the α-chain of fibrinogen on the gel (Figure 4A,B). We next sought to explore whether these two aptamers could also protect against native venom, which might contain additional related (or unrelated) proteins that could contribute to global fibrinogenolysis. Despite this possibility, our data showed that the aptamer ancrod-55 inhibited the fibrinogenolytic effect of *C. rhodostoma* venom on both the α- and β-chains, while batroxobin-26 aptamer prevented *B. atrox* venom-induced cleavage of the α-chain of fibrinogen (Figure 4C,D). These findings suggest that the binding specificities obtained during aptamer selection translate into inhibitory capabilities.
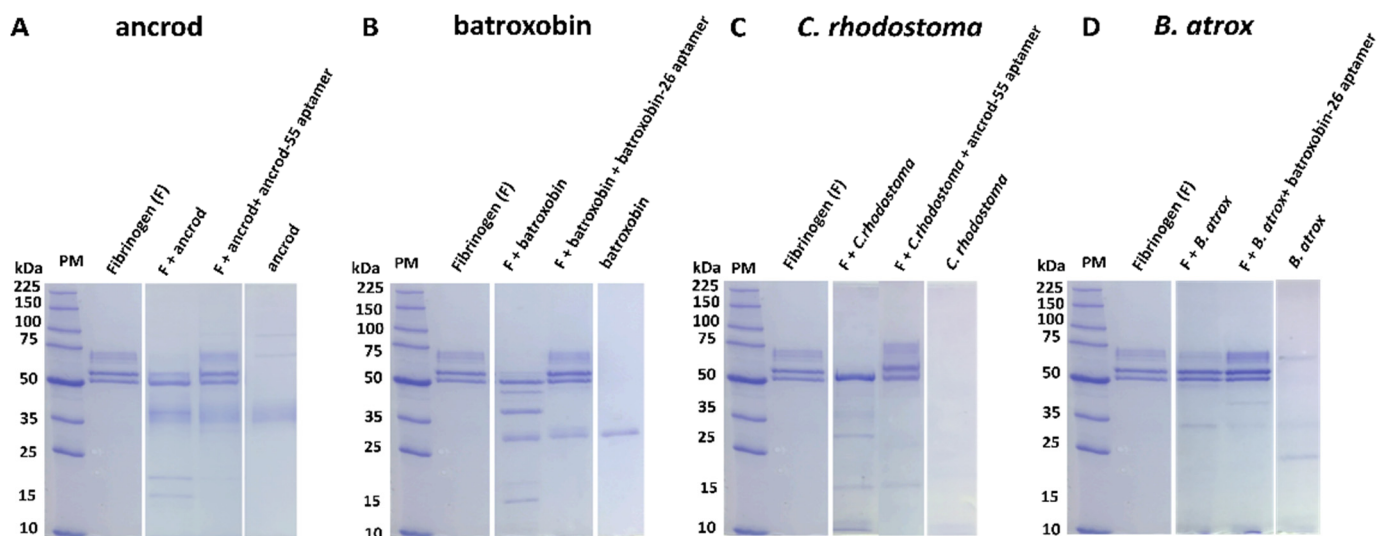

Figure 4. SDS-PAGE gel electrophoresis visualisation of fibrinogenolysis demonstrates that ssDNA aptamers directed against ancrod and batroxobin inhibit the fibrinogenolytic activity of recombinant toxins and the corresponding snake venoms. The fibrinogenolytic activity of: (**A**) ancrod and inhibition by the aptamer ancrod-55, (**B**) batroxobin and inhibition by batroxobin-26, (**C**) *C. rhodostoma* venom and inhibition by ancrod-55, and (**D**) *B. atrox* venom and inhibition by batroxobin-26. The figure shows a reduced 8% SDS-PAGE, visualised by Coomassie blue staining. All panels have the following layout: Lane 1, protein marker (PM); Lane 2, human plasma fibrinogen; Lane 3, toxin (ancrod or batroxobin) or venom (*C. rhodostoma* or *B. atrox*) + fibrinogen; Lane 4, toxin or venom + fibrinogen + aptamer (ancrod-55 or batroxobin-26, 1 pM); Lane 5, toxin or venom only.

The clotting time of diluted plasma with a standard thrombin concentration is inversely related to the fibrinogen concentration [80]. To further explore the inhibitory effect of the selected high-affinity aptamers against both SVSP toxins and native snake

venom, we measured fibrinogen depletion using native venom spiking experiments with platelet-poor plasma (PPP). Our results revealed that both ancrod and batroxobin, as well as native venom from *C. rhodostoma* and *B. atrox*, stimulate fibrinogen consumption in platelet-poor plasma (PPP), resulting in reductions versus the thrombin-stimulated saline control (<1.5 vs. 3.42 g/L) (Figure 5A). In both cases, however, the aptamers ancrod-55 and batroxobin-26 inhibited the depletion of fibrinogen stimulated by both toxins and native venoms to near control levels (2.7–2.9 vs. 3.42 g/L) (Figure 5A). Crucially, the aptamers showed highly comparable inhibitory potencies with those obtained with gold-standard commercial antivenoms, as evidenced by the resulting equivalent fibrinogen concentrations observed (Figure 5A).
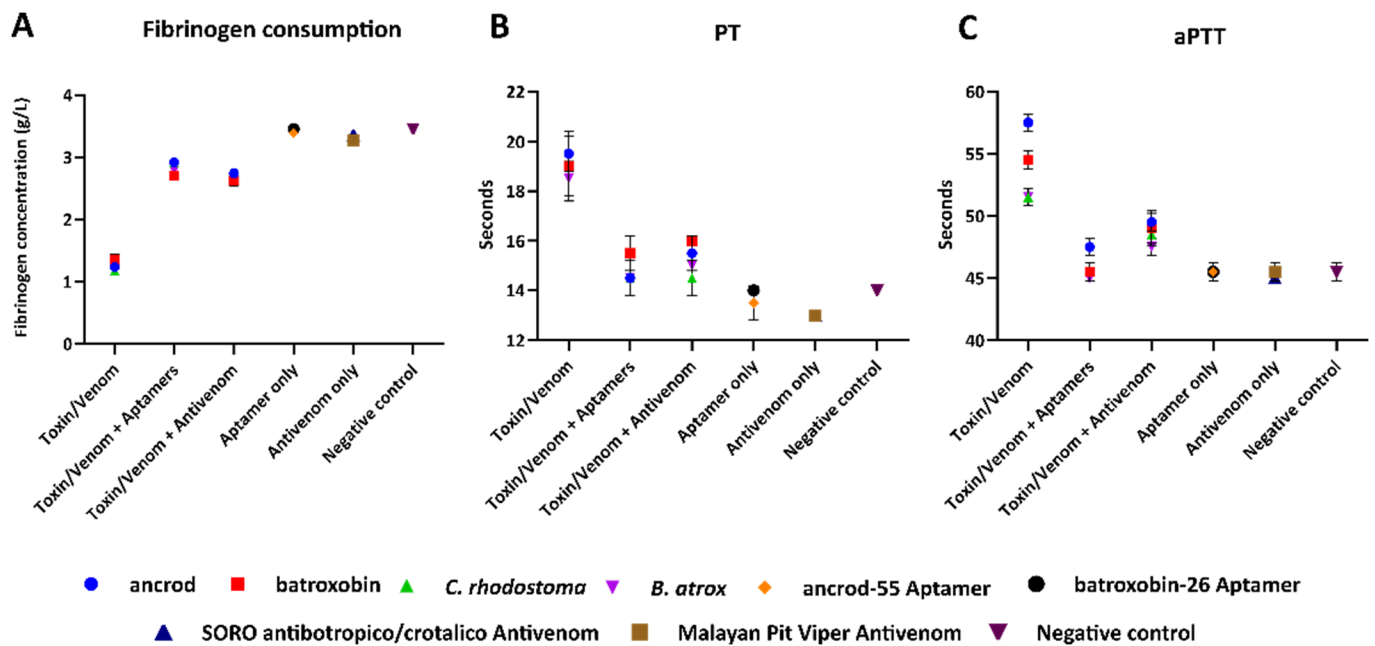

Figure 5. Fibrinogen consumption and prolongation of the PT and aPTT induced by recombinant toxins and corresponding snake venoms are reduced by the ssDNA aptamers in diluted citrated human PPP samples. (**A**) Fibrinogen concentrations were quantified using an excess of thrombin to convert fibrinogen to fibrin, (**B**) PT, which measures the combined effect of clotting factors of the extrinsic and common coagulation pathways (in seconds), and (**C**) aPTT, which measures the combined effect of the clotting factors of the intrinsic and common coagulation pathways. PPP samples were spiked with 0.6 ng of either recombinant toxin or native venom only (i.e., ancrod, batroxobin, *C. rhodostoma* or *B. atrox*); toxin/venom + 1 pM of specific aptamer (ancrod/*C. rhodostoma* with ancrod-55, batroxobin/*B. atrox* with batroxobin-26); or toxin/venom + 0.5 μg of specific commercial antivenom (ancrod/*C. rhodostoma* with Malayan pit viper antivenom, batroxobin/*B. atrox* with SORO antibotropico/crotalico antivenom). Controls consisted of aptamer-only samples, antivenom-only samples, and saline solution (negative control). Error bars represent the standard deviation (SD) of duplicate measurements.

2.5. Aptamers Reduce Toxin- and Venom-Induced Prolongations of Clotting Times

The prothrombin time (PT) measures the time for citrated plasma to clot and specifically assesses the clotting capability of extrinsic and common coagulation cascades. A prolonged PT can result from an absence or deficiency of one of the clotting factors X, VII, V, II or fibrinogen. Our recombinant toxin/native venom spiking experiments demonstrated that both ancrod and batroxobin and the corresponding venoms from *C. rhodostoma* and *B. atrox* resulted in a prolongation of the PT in PPP compared to the saline control (i.e., >18 vs. ~14 s, respectively) (Figure 5B). Noticeably, when co-incubated with the corresponding toxins/native venoms, the aptamers ancrod-55 and batroxobin-26 caused a substantial reduction in the PT compared with the toxin-only/native-venom-only samples, resulting

in the PT approaching the level of control readings (14.5–15.5 vs. ~14.0 s, respectively) and, thus, demonstrating the inhibition of toxin activity (Figure 5B). These reductions were highly comparable to those obtained with commercially available antivenoms (14–16 s).

We employed the activated partial thromboplastin time (aPTT) in the same manner as the PT, except, in this case, to measure clotting in the context of the combined effect of the intrinsic and common coagulation pathways (i.e., Factors II, V, VIII, IX, X, XI, XII and fibrinogen). Ancrod, batroxobin, *C. rhodostoma* venom and *B. atrox* venom all caused a prolongation of the aPTT in PPP when compared with the negative control (Figure 5C). The aptamers showed complete inhibition of toxin and native venom activity by reducing the aPTT to control levels, except for the ancrod and ancrod-55 aptamer combination, which showed substantial inhibition approaching control levels (ancrod, 57 s; ancrod + ancrod-55 aptamer, 48 s; normal control, 45 s) (Figure 5C). However, the aptamers slightly outperformed the levels of neutralisation obtained with commercial antivenoms. These findings are noteworthy when considering the differences in doses of these therapeutics (aptamer, 1 pM; antivenom, 4.55 pM).

3. Discussion

Though current antivenom treatments are life-saving therapeutics, they possess several limitations that restrict their clinical efficacy and utility for tackling tropical snakebites. Consequently, a variety of novel experimental approaches are currently being employed to develop new therapeutic interventions that circumvent these existing limitations with snakebite treatment. Next-generation antivenoms consisting of monoclonal antibodies (mAbs) selected for their desirable specificities show much promise in this regard, particularly since different antibody formats can be adapted to specific pharmacodynamic and pharmacokinetic needs [81]. However, to date, little effort has been devoted to exploring antibody alternatives despite outstanding concerns relating to the potential cost of mAb-based snakebite treatments. In other fields, ssDNA aptamers have emerged as promising alternatives to antibodies for both therapeutic applications and their use as diagnostic tools [38–40], and several ssDNA aptamers have been successfully selected and applied against a wide range of targets, including small molecules [82] and toxins [37,83–86]. Despite this prior research, ssDNA aptamers remain largely unexplored for their potential utility as snakebite therapeutics. Thus, in this proof-of-concept study, we sought to select ssDNA aptamers against fibrinogenolytic SVSP toxins found in medically important viper venoms and to evaluate their potential as novel toxin-inhibiting molecules via in vitro cross-reactivity and neutralisation studies.

Following fourteen cycles of SELEX selection, we selected two pools of aptamers directed against the recombinantly expressed SVSP toxins ancrod and batroxobin, which are found in native form in the venoms of the South East Asian pit viper *C. rhodostoma* and the South American lancehead pit viper *B. atrox*. Although the level of binding to each target increased steadily over SELEX selection cycles, by round 11, major increases in fluorescence intensity, indicating enrichment in binding to the target, occurred. Thereafter, counter-selection was employed to deplete binders directed towards the target carrier (beads), and two further cycles of enrichment were employed, ultimately resulting in highly comparable fluorescence intensity patterns obtained during the selection process for the two different targets. Sequencing 100 targets from the resulting two pools of ssDNA aptamers yielded thirteen and nine unique aptamers directed against ancrod and batroxobin, respectively, and analyses of the resulting dissociation constants enabled the selection of the highest affinity aptamers against each, which ultimately exhibited desirable low nanomolar K_ds (i.e., ancrod-55, 3.0 nM; batroxobin-26, 4.7 nM). These dissociation constants compare favourably with those obtained after ten rounds of diagnostic ssDNA aptamer selection against the neurotoxin β-bungarotoxin from the venom of *B. multicinctus* (>65.9 nm), for example [35].

Although ancrod and batroxobin are members of the same gene family (i.e., they are both snake venom serine proteases), they have different molecular masses (26–33 kDa)

and share only 67% amino acid sequence similarity [87]. Nonetheless, ALISA binding experiments demonstrated that the highest affinity aptamers selected and directed against one of these SVSP toxins were capable of cross-recognising and binding reciprocally to the other recombinant toxin under study here. Moreover, these experiments also revealed that both aptamers (i.e., ancrod-55 and batroxobin-26) were capable of binding to native toxins present in snake venoms that corresponded to the source of the recombinant toxins (i.e., *C. rhodostoma* and *B. atrox* venom) and, indeed, a broader variety of unrelated and distinct native snake venoms. Broadly speaking, each of the aptamers exhibited comparable moderate binding levels to each of the venoms tested, presumably via interaction with other SVSP toxins present within them, though ancrod-55 generally exhibited higher binding levels to these different venoms than batroxobin-26. However, we cannot rule out that non-specific interactions between the aptamers and other venom toxins might be contributing to the overall binding levels obtained in these experiments.

Both ancrod and batroxobin are coagulopathic SVSP toxins capable of stimulating fibrinogen consumption and prolonging clotting times [13,15,16]. Indeed, most SVSPs are fibrinogenolytic enzymes that result in the depletion of circulating fibrinogen during envenoming. Using a panel of in vitro bioassays, we demonstrated that recombinant ancrod and batroxobin used for aptamer selection exhibit functional activities consistent with native toxins, including fibrinogenolytic activity via cleavage of the α-chain of fibrinogen, the reduction of fibrinogen plasma concentrations, and the prolongation of clotting times in PT and aPTT assays. Crucially, the coincubation of the ssDNA aptamers with the corresponding recombinant toxins abolished the cleavage of fibrinogen and reduced the consumption of fibrinogen in human plasma samples to control levels, demonstrating that the binding observed translates into a degree of functional inhibition. Similar results were observed when measuring the PT and aPTT in toxin-spiked platelet-poor plasma, with the homologous aptamers reducing the prolongation of clotting times stimulated by each toxin to near control levels. The inhibition also extended to native snake venoms, with the aptamers inhibiting their fibrinogenolytic and delayed clotting time effects in a highly comparable manner to those obtained with the recombinant toxins. These findings suggest that SVSP toxins likely dominate the fibrinogenolytic effect of *C. rhodostoma* and *B. atrox* venoms and are effectively inhibited by the ssDNA aptamers ancrod-55 and batroxobin-26, though we cannot rule out some contributory interactions between the aptamers and distinct coagulopathic toxins found in these venoms. Irrespectively, it is worth noting that the toxin inhibitory activities demonstrated here by the selected high-affinity aptamers are potent, with low concentrations (1 pM) inhibiting toxin and venom activities observed across the various assays, which compares very favourably to the doses required by the conventional polyclonal antivenoms to effect comparable neutralisation (4.55 pM).

Future work should explore whether the in vitro inhibitory data obtained here might translate into in vivo protection against venom-induced toxicity in preclinical animal models or whether toxin-family-directed aptamers, such as those identified here, need to be combined with other inhibitory molecules (i.e., other aptamers or different inhibitory molecules such as mAbs or small molecule drugs) targeting distinct toxin families to prevent severe envenoming pathology in vivo [6]. This latter point seems highly likely, given that snake venoms contain multiple isoforms from different toxin families that often work in concert to cause pathological effects [6,7]. There is, therefore, a clear trade-off between the toxin-specificity of an inhibitory molecule and the number of inhibitors (whether they be aptamers or mAbs) required to neutralise whole venom, where increased inhibitory breadth against additional toxin isoforms is likely to correspond to some degree of reduction in affinity and/or inhibitory potency against broader targets. Further, increasing the breadth of toxin recognition seems likely to increase the risk of off-target interactions; thus, it is important that aptamer-based therapeutics are also assessed for their potential to interact with cellular receptors or cognate proteins in vitro and evaluated for their potential toxicity in vivo in relevant preclinical models. Such experimental approaches will be key

to understanding the number of distinct, well-tolerated aptamers required to neutralise a breadth of snake venoms.

Nonetheless, the proof-of-concept findings described here reveal that rationally selected ssDNA aptamers hold great value for exploration as novel inhibitory molecules capable of broadly inhibiting snake venom toxins such as SVSPs. However, the therapeutic potential of aptamers does not come without several challenges. One major limitation is that ssDNA aptamers are susceptible to nucleases and this, combined with their small size, results in short half-lives in vivo, which can be as low as two minutes due to DNA degradation and rapid clearance [49]. However, aptamers also possess great flexibility and can be modified to increase their stability and their resulting half-life, with conjugation to a higher molecular mass protein carrier, for example, liposomes, cholesterol or PEG; this has previously been demonstrated to successfully decrease the clearance rate from plasma to acceptable levels, though, it adds to cost of goods [57,59,88]. Other limitations include the initial selection process often being labour-intensive and time-consuming, though the downstream production of the resulting identified ssDNA aptamers offers several advantages over mAb production, for example, due to their size and chemical synthesis. Finally, to date, it is worth re-emphasising that only a single aptamer has passed through an FDA-approval process (Macugen® (Pegaptanib)) [62], and as such, regulatory challenges are likely to remain for exploiting ssDNA aptamers as new therapeutics.

Despite these limitations, aptamers possess several clear advantages in terms of therapeutic characteristics over the polyclonal antibodies currently used for treating snakebite. For example, aptamers are chemically synthesised and, thus, do not require the use of ethically and financially costly experimental animals, and the resulting product exhibits a relative lack of batch-to-batch variation, unlike biologic antivenom [89]. Further, aptamers exhibit desirable stability and are likely more resistant to harsh conditions than antibodies [90], which may be of particular benefit in cold-chain-unstable parts of the tropics that suffer a high burden of snakebite. Finally, the large-scale cost of manufacturing aptamers seems likely to be relatively inexpensive compared with existing polyclonal antivenoms. Currently, manufacturing costs for aptamers range from USD 140–280 per dose [88], and while the dose efficacy of aptamers in the context of snakebite remains to be established, it seems likely that aptamer-based treatments could reduce the high costs currently borne by tropical snakebite victims, which often exceed USD 1000 in sub-Saharan Africa, for example [31]. Although much work needs to be undertaken before such benefits can be realised, the proof-of-concept data described herein add further weight to the potential utility of aptamers as future snakebite treatments and strongly advocate for their continued exploration as a novel therapeutic modality for inhibiting pathogenic snake venom toxins.

4. Materials and Methods

4.1. DNA Library and Primer Design

The DNA library and PCR primers were chemically synthesised and purified by Integrated DNA Technologies, Inc. The random ssDNA library used in the first SELEX cycle consisted of 2×10^{17} sequences, specifically containing a central random region of 40 nucleotides flanked by two primers consisting of 16 nucleotides at the 5′ and 3′ ends (5′-TCCCTACGGCGCTAAC-N40-GTTGTAGCACGGTGGC-3′) for amplification of the library sequence. To facilitate the separation of ssDNA from amplified dsDNA PCR products and to quantify DNA during selection, the forward and reverse primers were designed and modified with fluorescein and a HEG linker (the spacer is designed to block the PCR extension step during amplification). The modified PCR forward primer used during the selection cycles was 5′-6-FAM-TCCCTACGGCGCTAAC-3′ and the reverse primer was (5′-poly dA20-HEG-spacer-GTTGTAGCACGGTGGC-3′). An unmodified primer set was used for PCR amplification and cloning when SELEX rounds were completed and enriched.

4.2. Target Conjugation

The recombinant toxins used in this study, ancrod from *C. rhodostoma* (UniProt: P26324) and batroxobin from *B. atrox* (UniProt: P04971), were previously expressed in HEK293 mammalian cell lines [76]. In this study, we used these toxins to conjugate to NHS (N-hydroxysuccinimide)-activated Sepharose® 4 Fast Flow beads (Sigma-Aldrich, Dorset, UK) to generate ssDNA aptamers as novel toxin-inhibiting therapeutics. To do so, the manufacturer's protocol was followed. First, a 300 µg/mL solution of each toxin was prepared in coupling buffer (0.1 M NaHCO$_3$, 0.5 M NaCl, pH 8.3). Next, 2 mL of NHS-activated Sepharose beads were rinsed multiple times with 1 mM HCl for 15 min to remove the additives and preserve the activity of the reactive groups. Each venom toxin was then added immediately to the washed Sepharose beads independently (1:1 *v:v* ratio) and mixed by end-over-end rotation overnight at 4 °C. After incubation, the beads were centrifuged at 14× *g* for 5 min, the supernatant discarded, and the samples washed with 1 mL of 1 M NaCl. This centrifugation step was repeated before 2 mL of 1 M NaCl was added, and the samples were incubated with rotation for 2 h at 4 °C to block the unreacted amine groups on the beads. After blocking, the toxin-conjugated Sepharose was washed three times with 4 mL in an alternating manner, first with 0.1 M acetic acid/sodium acetate, pH 4, containing 0.5 M NaCl 0.1 M, followed by Tris-HCl buffer, pH 8, containing 0.5 M NaCl. Thereafter, the toxin-conjugated Sepharose was stored in 50 mM Tris-HCl buffer (pH 7.5), 0.05% sodium azide at 4 °C until use.

4.3. PCR Amplification

Each of the recombinant toxin-conjugated Sepharose mixtures was washed five times by adding 500 µL binding buffer (50 mM Tris-HCl, pH 7.5, 150 mM NaCl, 2 mM MgCl$_2$) to 100 µL of Sepharose using centrifugal tube filters (0.45 µm) (Costar, Washington, DC, USA). In the first SELEX cycle, 50 µL (3 nM) of the DNA library solution in a 450 µL binding buffer was used, whereas 50 pM of the DNA elution from each round was used for subsequent cycles. The DNA and binding buffer mixture were heated to 90 °C on a heat block for five minutes, cooled at 4 °C for ten minutes and then held at room temperature (RT) for five minutes. Next, 300 µL of DNA and binding buffer mixture was added to the washed beads and incubated end-over-end for 1 h at RT. After incubation, the mixtures were washed and centrifuged five times with 500 µL of binding buffer at 82× *g* for 2 min to ensure the elimination of unbound DNA. The flow-through from the first wash was retained for use as a positive control in downstream 2% agarose gel electrophoresis and PAGE experiments. DNA bound to the toxin-conjugated beads was collected from each sample using elution buffer (7 M urea in binding buffer) and incubated at 90 °C for 10 min on a heat block. The elution step has performed a total of five times via the addition of 300 µL elution buffer until no fluorescence was detected in the eluted aliquots, indicating the complete elution of bound DNA from the beads. The eluted aliquots were then desalted with filtered water and concentrated using an ultrafiltration device with a 3 kDa cut-off membrane (Amicon Ultra-0.5 Centrifugal Filter Unit; Merck, Dorset, UK) to remove any urea and salt residues.

A dsDNA product with different lengths for each strand was generated via PCR amplification by using two parallel 50 µL reactions (one for each toxin target), each containing five units of Taq Plus and polymerase buffer (New England, BioLabs®, Hitchin, UK), 2 mM MgCl$_2$, 200 µM deoxyribonucleotide triphosphate (dNTP) and 0.2 µM of the unmodified forward and reverse primers. The PCR conditions were: 94 °C for 10 min, followed by 17 cycles of 94 °C for 1 min, 54 °C for 1 min and 72 °C for 1 min, and a final extension step of 10 min at 72 °C. To confirm the amplification of the dsDNA product, the samples were then analysed electrophoretically using 2% agarose gel electrophoresis.

An ssDNA product with different lengths for each strand was also generated via PCR amplification using 20 parallel 50 µL reactions using the same conditions as outlined above, except with the use of 0.2 µM of the labelled forward primer. Following amplification, the 20 reactions were pooled and aliquoted into three Eppendorf tubes, each containing 250 µL of pooled ssDNA product, 50 µL 3 M sodium acetate, pH 5.2 and 750 µL absolute ethanol.

The tubes were then mixed and stored at $-80\ ^\circ$C for 2 h before centrifugation at $13,000\times g$ for 30 min at 4 $^\circ$C. The supernatant was discarded, and the remaining pellet was dried at 90 $^\circ$C for a couple of minutes on a heat block before resuspension in 400 μL of water and formamide (1:1 v/v) and incubation at 90 $^\circ$C for 5 min.

4.4. Separation of ssDNA by Denaturing PAGE

We employed a 10% denaturing PAGE to separate the resulting ssDNA from the double-stranded (dsDNA) amplified PCR products. Fifty microlitres of each dsDNA sample were independently loaded into the gel and run at 200 volts for 55 min using a Mini-PROTEAN electrophoresis system (Bio-Rad, Hertfordshire, UK). Next, the ssDNA band was observed under UV light, dissected, cut and transferred to a 15 mL falcon tube containing 4 mL of Tris-ethylenediaminetetraacetic acid (EDTA) buffer solution (TE buffer; 10 mM Tris-HCl, pH 7.4, 1 mM EDTA). Samples were then subjected to freeze–thaw for 30 min at $-80\ ^\circ$C, 10 min at 90 $^\circ$C, followed by incubation on a rotary shaker overnight at 37 $^\circ$C [91]. Finally, ssDNA was eluted and concentrated using an ultrafiltration device with a 3 kDa cut-off membrane (Amicon Ultra-0.5 Centrifugal Filter Unit; Merck, Dorset, UK), as described earlier. The UV and fluorescence intensity of each dsDNA and ssDNA were then measured for each eluted fraction using a NanoDrop 2000 C spectrophotometer and a FLUOstar Omega 384 well black assay plate reader (B.M.G. LabTech), respectively. The fluorescence spectra were detected at an excitation wavelength of 470 nm and an emission of 515 nm.

4.5. Counter-Selection

Following enrichment, counter-selection (negative selection) was employed using blank Sepharose beads instead of those conjugated to toxins. The objective was to increase enrichment to the toxin target via the elimination of aptamers directed towards the beads. Sepharose beads were subjected to the aforementioned conjugation process with 0.1 M Tris-HCl buffer, pH 8.3, containing 0.5 M NaCl only (i.e., in the absence of toxins), and counter-selection followed the same experimental strategy described above and was used to filter out negative targets.

4.6. Cloning and Sequencing ssDNA Aptamers

After ssDNA recovery, the eluted ssDNA from the 14th round of selection was amplified using the unlabelled PCR primer (5′-TCCCTACGGCGCTAAC-3′), following the same conditions as PCR amplification: 94 $^\circ$C for 10 min, followed by 17 cycles of 94 $^\circ$C for 1 min, 54 $^\circ$C for 1 min and 72 $^\circ$C for 1 min, and a final extension step of 10 min at 72 $^\circ$C. Next, ligation was performed using the TOPO TA Cloning Kit for Sequencing and One Shot TOP10 Chemically Competent E. coli (Thermo-Fisher Scientific, Altrincham, UK). Ligation reactions consisted of 2 μL of fresh PCR product, 1 μL of salt solution, 1 μL of TOPO® vector and 1 μL of nuclease-free water, with the resulting samples mixed gently and incubated for 30 min at RT (20–25 $^\circ$C). For cloning, 5 μL of the ligated product was added to a vial of One Shot TOP10 Chemically Competent E. coli (Thermo-Fisher Scientific, Altrincham, UK) and mixed gently. The cells were then placed on ice for 30 min, heat-shock-treated for 30 s at 42 $^\circ$C and transferred back to ice. Next, 250 μL of pre-warmed S.O.C medium was added, and samples were incubated at 37 $^\circ$C for 1 h with horizontal shaking at 200 rpm. Thereafter, 50 μL of the medium was spread on 25 mL of Lauria Broth (LB) agar (VWR, Leicestershire, UK) plates supplemented with 25 μL ampicillin (20 mg/mL) (Sigma-Aldrich, Dorset, UK), 250 μL 5-bromo-4-chloro-3-indolyl-β-D-galactoside (X-Gal) (20 mg/mL) (Sigma-Aldrich, Dorset, UK) and IPTG 25 μL (100 mM) (Sigma-Aldrich, Dorset, UK) and incubated at 37 $^\circ$C overnight. Following incubation, ten random positive colonies (white colonies) were picked for colony PCR analysis: 5 μL 10 × PCR buffer, 0.5 μL dNTPs mix (50 mM), 0.5 μL of M13 forward primer (5′-GTAAAACGACGGCCAGT-3′) and M13 reverse primer (5′-CAGGAAACAGCTATGAC-3′) (0.1 μg/μL each), 41.5 μL nuclease-free water and 1 μL Taq polymerase (1 unit/μL). Colony PCR was performed using the following cycling pa-

rameters: initial denaturation at 94 °C for 2 min, followed by 25 cycles of denaturation at 94 °C for 1 min, annealing at 55 °C for 1 min and extension at 72 °C for 1 min, with a final extension step at 72 °C for 7 min. To confirm insert amplification, 2% agarose gel electrophoresis was performed.

One hundred positive bacterial colonies were sterilely selected and inoculated with 5 mL of LB medium containing 50 μL ampicillin (20 mg/mL) and incubated overnight at 37 °C with shaking at 200 rpm. Next, plasmid DNA was purified using a QIAprep Spin Miniprep Kit (Qiagen, Düsseldorf, Germany). The overnight culture was centrifuged at $6000 \times g$ for 10 min at RT. The pellet was then resuspended in 250 μL Buffer P1 (with Rnase A) and transferred to a microcentrifuge tube. Then, 250 μL Buffer P2 was added and mixed thoroughly by inverting the tube gently 4–6 times. After that, 350 μL Buffer N3 was added and mixed immediately and thoroughly by inverting the tube 4–6 times. Next, samples were centrifuged for 10 min at $17,900 \times g$, and the supernatant was transferred to QIAprep 2.0 Spin Columns before brief centrifugation at $2817 \times g$ for one minute with the eluate discarded. Columns were then washed with 750 μL Buffer PE via centrifugation at $2817 \times g$ for one minute, the eluate discarded, and columns centrifuged for an additional minute to remove any residual buffer. Finally, 50 μL Buffer EB (10 mM Tris-HCl, pH 8.5) was added to each column and incubated at RT for two minutes prior to elution via centrifugation at $2817 \times g$ for 1 min. The resulting PCR products were then sequenced commercially via Sanger sequencing (SourceBioScience, Nottingham, UK), and the resulting ssDNA aptamer sequences were analysed and aligned using PRALINE [92].

4.7. Dissociation Constants

The binding affinities of the identified ssDNA aptamers against each of the corresponding toxins used for selection were evaluated using a fluorescence-based assay. Both forward and reverse primer-binding sites were truncated and labelled with 6-FAM (fluorescein-labelled) before synthesis. Different concentrations of fluorescein-labelled ssDNA aptamer (0, 5, 10, 50, 100, 200, 300 and 400 nM) were incubated with a constant amount of the corresponding toxin-conjugated beads (50 μL), as described in the selection protocol (by heating to 90 °C for 10 min, 4 °C for 10 min and then at RT for 5 min). After 1 h of incubation at RT with rotation, the unbound ssDNA aptamers were washed using 3 kDa centrifuge filters and 500 μL binding buffer, and the toxin-bound ssDNA aptamers were eluted five times via the addition of 300 μL elution buffer (7 M urea in binding buffer) and incubation at 90 °C for 10 min on a heat block. The five eluted aliquots were then concentrated using an ultrafiltration device with a 3 kDa cut-off membrane (Amicon Ultra-0.5 Centrifugal Filter Unit; Merck, Dorset, UK) and desalted with filtered water to remove urea and salts. The fluorescence intensity of each ssDNA was then measured for each eluted fraction at an excitation wavelength of 470 nm and an emission of 515 nm. The K_d of each ssDNA aptamer was calculated via nonlinear regression analysis of the resulting plotted hyperbolic curves using Prism v8 software (GraphPad).

4.8. Binding by ALISA

To quantify reciprocal binding to the recombinant toxins (ancrod and batroxobin) by the highest affinity aptamers (determined by the K_d analysis above), we used an ALISA assay. We also assessed binding to native venom samples that corresponded to the source of each toxin (i.e., *C. rhodostoma*, captive-bred and *B. atrox*, Brazil) and an additional panel of eleven geographically and taxonomically diverse snake species (*Bitis arietans*, Nigeria; *Bothrops asper*, Costa Rica; *Bothrops jararaca*, Brazil; *Crotalus atrox*, captive-bred; *Daboia russelii*, Sri Lanka; *Deinakgistrodon acutus*, captive-bred; *Dispholidus typus*, South Africa; *Echis carinatus*, India; *Echis ocellatus*, Nigeria; *Rhabdophis subminiatus*, Hong Kong; *Trimeresurus albolabris*, captive-bred) to assess the breadth of binding. Many of these venoms were collected from animals maintained under controlled environmental and dietary conditions in the UK-Home-Office-licensed and -inspected herpetarium of the Centre for Snakebite Research and Interventions (CSRI) at the Liverpool School of Tropical Medicine (LSTM). The

remainder were sourced from historical venom collections held in the CSRI herpetarium (specifically, *B. asper*, *B. jararaca*, *C. rhodostoma*, *D. russelii*, *E. carinatus*, *R. subminiatus* and *T. albolabris*) or commercially purchased from Latoxan, France (*D. typus*). Lyophilised venoms were stored at 4 °C and reconstituted with phosphate-buffered saline (PBS) (0.12 M NaCl, 0.04 M phosphate, pH 7.2) to a concentration of 1 mg/mL prior to use.

For the ALISA, 1 μL of Modifier reagent (HRP Conjugation Kit—Lightning-Link®, ab102890) (Abcam, Waltham, MA, USA) was added to 10 μL of each ssDNA aptamer (ancrod-55 and batroxobin-26; 200 nM), mixed gently and left standing for 3 h in the dark at RT (20–25 °C). After incubation, 1 μL of Quencher reagent (HRP Conjugation Kit—Lightning-Link®, ab102890) was added to each ssDNA aptamer sample and mixed gently. Next, microtiter 96-well ELISA plates (Greiner Bio-One; Thermo-Fisher Scientific, Dorset, UK) were coated with coating buffer (100 mM carbonate/bicarbonate buffer, pH 9.6) containing 100 ng of each toxin or native venom and incubated overnight at 4 °C. Plates were then washed three times with PBST (1× PBS, pH 7.4 containing 0.1% Tween) before blocking with 300 μL/well of 0.5% bovine serum albumin (BSA; Sigma-Aldrich, Dorset, UK) diluted in PBS (filtered with MF-Millipore® Membrane Filter, 0.45 μm pore size). Following incubation at RT for two hours, the plates were washed another three times with PBST. Next, two concentrations of the aptamers were prepared and diluted in nuclease-free water (2 and 0.4 nM). Then, 100 μL of each aptamer, alongside water (as a negative control), was added to the plate in duplicate, followed by incubation for 2 h at RT. The plates were then rewashed three times with PBST before the addition of the 3,3′,5,5′-Tetramethylbenzidine (TMB) Liquid Substrate System for ELISA (Sigma-Aldrich, Dorset, UK) and incubated for 12 min in the dark at RT. To stop the reaction, 25 μL of 20% sulphuric acid was added before the signal was read spectrophotometrically at 450 nm on a FLUOstar Omega microplate reader. Finally, all reads at 450 nm were subtracted from 540 nm to remove any background signal.

4.9. Visualisation of Fibrinogenolysis via SDS-PAGE Gel Electrophoresis

To assess the capability of the selected ssDNA aptamers to inhibit the fibrinogenolytic activity of the recombinant toxins and the corresponding native snake venoms, we used an SDS-PAGE approach. The toxins ancrod and batroxobin (3 μg, 1 mg/mL), and the corresponding venoms from *C. rhodostoma* and *B. atrox* (1.05 μg, 0.3 mg/mL), were incubated with human plasma fibrinogen (3.75 μg, 2.5 mg/mL, Sigma-Aldrich, Dorset, UK) for two hours at 37 °C. The same samples were also used in neutralisation experiments following a preincubation step at 37 °C for 15 min with each of the selected ssDNA aptamers (1 pM). Next, all samples were incubated for two hours at 37 °C. Human plasma fibrinogen with PBS instead of venom was used as the negative control. After incubation, 10 μL of each sample was mixed at a 1:1 *v/v* with reducing buffer (3.55 μL H_2O, 1.25 mL 0.5 M Tris-HCl (pH 6.8), 2.50 mL glycerol, 2.0 mL 10% SDS, 1.50 mL saturated bromophenol blue and 150 μL β-mercaptoethanol) and heated for 5 min at 100 °C. For gel electrophoresis, ten well 8% SDS-PAGE were hand-cast, using the following approach: 10 mL resolving gel (4.7 mL H_2O, 2.5 mL Tris-HCl pH 8.8 (1.5 M), 2.7 mL 30% bis-acrylamide, 50 μL 20% SDS, 100 μL 10% ammonium persulfate (APS) and 7 μL tetramethylethylenediamine (TEMED)); 4 mL of 4% stacking gel (2.7 mL H_2O, 0.5 mL Tris-HCl pH 6.8 (1 M), 800 μL 30% bis-acrylamide, 20 μL 20% SDS, 40 μL 10% APS and 4 μL TEMED). Next, 10 μL of each sample, alongside 5 μL of broad molecular mass protein marker (Broad Range Molecular Marker, Promega), was loaded onto the gel and run at 200 volts for 55 min using a Mini-PROTEAN electrophoresis system (Bio-Rad, Hertfordshire, UK). Resulting gels were then stained at a final concentration of 0.1% (*w/v*) Coomassie blue R350 (0.4 g of Coomassie blue R350 in 200 mL of 4% (*v/v*) methanol in H_2O), 10% (*v/v*) acetic acid and 20% (*v/v*) methanol overnight at RT. Gels were destained (4:1:5 methanol: glacial acetic acid: H_2O) for at least two hours at RT. For visualisation, gels were imaged using a Gel Doc EZ Gel Documentation System (Bio-Rad, Hertfordshire, UK).

4.10. Sample Preparation for Clotting Profiling Experiments

Blood samples for clotting profiling experiments were obtained according to ethically approved protocols (LSTM research tissue bank, REC ref. 11/H1002/9) from consenting healthy volunteers who confirmed they had not taken any anticoagulant treatments for at least three months prior to blood collection. Blood samples were collected in tubes containing acid citrate dextrose adenine (ACD-A) as an anticoagulant. To prepare fresh frozen plasma (FFP) a fresh blood sample was centrifuged at $2500\times g$ at 20–25 °C for 10 min, and the supernatant was retained and stored at -80 °C until use. Platelet-poor plasma (PPP) was then generated by centrifuging the FFP samples again in an identical manner, with the resulting platelet-depleted supernatant stored at -80 °C until further use.

In addition to the samples prepared above, we also used commercially sourced samples (Diagnostic Reagents Ltd., Thame, UK) to serve as quality control checks for the various reagents employed. To this end, normal and abnormal test controls were implemented for the experiments described below prior to experimentation. These consisted of (1) Diagen control plasma for fibrinogen: normal (RCPN070) and abnormal (RCPA080) and (2) control plasma for aPTT and PT: normal (IQCN130), abnormal 1 (Mild, IQCM140) and abnormal 2 (Severe, IQCS150). All QC samples were aliquoted into 500 µL, stored at -80 °C, and defrosted in a water bath for 5 min at 37 °C immediately prior to use. To act as positive controls for the aptamers, we used commercial antivenoms, specifically the Thai Red Cross monovalent equine Malayan pit viper antivenom (Lot #: CR00316, expiry date 06/2021) for ancrod and *C. rhodostoma* experiments and the Instituto Butantan polyvalent equine SORO antibotropico/crotalico antivenom (Lot #: 1012308, expiry date: 2013) for batroxobin and *B. atrox* experiments. These freeze-dried antivenoms were reconstituted in the pharmaceutical-grade water supplied by the manufacturers, the protein concentrations quantified using a NanoDrop (Thermo-Fisher Scientific, Dorset, UK), and then stored at 4 °C in the short term until use.

4.11. Fibrinogen Consumption via the Clauss Method

The Clauss method is a quantitative, clot-based assay. It measures the ability of thrombin to convert fibrinogen to fibrin clots, followed by manual time measurements of clotting [80]. Here, we applied this method in toxin- and venom-spiking experiments to assess the inhibitory capability of the selected ssDNA aptamers against the depletion of fibrinogen. Twenty microlitres of PPP were spiked with 0.6 ng of ancrod, batroxobin, *C. rhodostoma* or *B. atrox* venom, or 0.9% saline solution as the negative control. All samples were also repeated in the presence of 1 pM of the selected ssDNA aptamers or 0.5 µg of the commercial antivenoms following preincubation at 37 °C for 5 min. Samples were then diluted tenfold with 0.02 M imidazole buffer (pH 7.35), transferred to glass test tubes (10 × 75 mm), and warmed at 37 °C for 120 s. Thereafter, 100 µL of thrombin reagent (20 units/mL) (Diagnostic Reagents Ltd., Thame, UK) was added and time measurements commenced. Tubes were gently tilted at regular intervals (returning to the water bath between tilting), and the time for the formation of a clot was recorded. All experiments were performed in duplicate.

4.12. Prothrombin Time (PT)

To measure the inhibitory capability of selected aptamers against toxins acting on the extrinsic coagulation pathway, we quantified differences in the PT between toxin and venom samples in the presence and absence of aptamers. Measurements of PT were undertaken by first adding 100 µL of calcium rabbit brain thromboplastin (Diagnostic Reagents Ltd., Thame, UK) to a glass test tube (10 × 75 mm) and incubating at 37 °C for 60–120 s in a water bath. Next, 50 µL of PPP was spiked with 50 µL containing 0.6 ng of ancrod, batroxobin, *C. rhodostoma* or *B. atrox* venom, or saline solution as the negative control. All samples were also repeated in the presence of 1 pM of the selected ssDNA aptamers or 0.5 µg of the commercial antivenoms, following preincubation at 37 °C for 5 min. Time measurements were commenced, tubes were gently tilted at regular intervals

(returning to the water bath between tilting), and the time for the formation of a clot was recorded. All experiments were performed in duplicate.

4.13. Activated Partial Thromboplastin Time (aPTT)

To measure the inhibitory capability of selected aptamers against toxins acting on the intrinsic and common coagulation pathways, we quantified differences in the aPTT between toxin and venom samples in the presence and absence of aptamers. To do so, 50 µL of Micronised Silica/Platelet Substitute Mixture (Diagnostic Reagents Ltd., Thame, UK) was placed in glass test tubes (10 × 75 mm) in a water bath at 37 °C and incubated for 60–120 s. Next, 50 µL of PPP was spiked with 0.6 ng of ancrod, batroxobin, *C. rhodostoma* venom or *B. atrox* venom, or saline solution as the negative control. All samples were also repeated in the presence of 1 pM of the selected ssDNA aptamers or 0.5 µg of the commercial antivenoms, following preincubation at 37 °C for 5 min. Thereafter, samples were added to the glass test tubes and gently tilted at regular intervals for precisely five minutes at 37 °C. Finally, 50 µL of 25 mM calcium chloride (preincubated at 37 °C) was added to each tube, and the tube was gently tilted until the resulting clot time was recorded. All experiments were performed in duplicate.

Author Contributions: N.A., N.R.C. and M.Z. designed the study. N.A. and N.R.C. chose and provided the target analyte. R.C. planned the SELEX experiments. N.A. and R.C. carried out the SELEX and DNA sequencing experiments. J.A. planned the ALISA experiments. N.A. performed all other experiments and analysed the data. N.A. and N.R.C. wrote the manuscript with input from all other authors. All authors have read and agreed to the published version of the manuscript.

Institutional Review Board Statement: Human plasma samples were collected under ethical permissions granted to the LSTM research tissue bank under LSTM research ethics committee ref. # 11/H1002/9.

Informed Consent Statement: Informed consent was obtained from all subjects involved in the study.

Data Availability Statement: The data presented in this study are available in this article.

Conflicts of Interest: The authors declare no known competing financial interests or personal relationships that could have appeared to influence the work reported in this paper.

References

1. Alirol, E.; Sharma, S.K.; Bawaskar, H.S.; Kuch, U.; Chappuis, F. Snake bite in South Asia: A review. *PLoS Negl. Trop. Dis.* **2010**, *4*, e603. [CrossRef] [PubMed]
2. Gutiérrez, J.M.; Calvete, J.J.; Habib, A.G.; Harrison, R.A.; Williams, D.J.; Warrell, D.A. Snakebite envenoming. *Nat. Rev. Dis. Primers* **2017**, *3*, 17063. [CrossRef] [PubMed]
3. Kasturiratne, A.; Wickremasinghe, A.R.; de Silva, N.; Gunawardena, N.K.; Pathmeswaran, A.; Premaratna, R.; Savioli, L.; Lalloo, D.G.; de Silva, H.J. The global burden of snakebite: A literature analysis and modelling based on regional estimates of envenoming and deaths. *PLoS Med.* **2008**, *5*, e218. [CrossRef]
4. Chippaux, J.-P. Snakebite envenomation turns again into a neglected tropical disease! *J. Venom. Anim. Toxins Incl. Trop. Dis.* **2017**, *23*, 38. [CrossRef] [PubMed]
5. Laxme, R.S.; Khochare, S.; de Souza, H.F.; Ahuja, B.; Suranse, V.; Martin, G.; Whitaker, R.; Sunagar, K. Beyond the 'big four': Venom profiling of the medically important yet neglected Indian snakes reveals disturbing antivenom deficiencies. *PLoS Negl. Trop. Dis.* **2019**, *13*, e0007899.
6. Casewell, N.R.; Jackson, T.N.W.; Laustsen, A.H.; Sunagar, K. Causes and consequences of snake venom variation. *Trends Pharmacol. Sci.* **2020**, *41*, 570–581. [CrossRef]

7. Slagboom, J.; Kool, J.; Harrison, R.A.; Casewell, N.R. Haemotoxic snake venoms: Their functional activity, impact on snakebite victims and pharmaceutical promise. *Br. J. Haematol.* **2017**, *177*, 947–959. [CrossRef]

8. Lu, Q.; Navdaev, A.; Clemetson, J.M.; Clemetson, K.J. Snake venom C-type lectins interacting with platelet receptors. Structure–function relationships and effects on haemostasis. *Toxicon* **2005**, *45*, 1089–1098. [CrossRef]

9. White, J. Snake venoms and coagulopathy. *Toxicon* **2005**, *45*, 951–967. [CrossRef]

10. Warrell, D.A. Snake bite. *Lancet* **2010**, *375*, 77–88. [CrossRef]

11. Gutiérrez, J.M.; Vargas, M.; Segura, A.; Herrera, M.; Villalta, M.; Solano, G.; Sánchez, A.; Herrera, C.; León, G. In vitro tests for assessing the neutralizing ability of snake antivenoms: Toward the 3Rs principles. *Front. Immunol.* **2021**, *11*, 617429. [CrossRef] [PubMed]

12. Isbister, G.K. (Ed.) Snakebite doesn't cause disseminated intravascular coagulation: Coagulopathy and thrombotic microangiopathy in snake envenoming. In *Seminars in Thrombosis and Hemostasis*; Thieme Medical Publishers: New York, NY, USA, 2010.

13. Ainsworth, S.; Slagboom, J.; Alomran, N.; Pla, D.; Alhamdi, Y.; King, S.I.; Bolton, F.; Gutiérrez, J.M.; Vonk, F.J.; Toh, C.H.; et al. The paraspecific neutralisation of snake venom induced coagulopathy by antivenoms. *Commun. Biol.* **2018**, *1*, 34. [CrossRef] [PubMed]

14. Phillips, D.J.; Swenson, S.D.; Francis, S.; Markland, J.; Mackessy, S. Thrombin-like snake venom serine proteinases. *Handb. Venoms Toxins Rep.* **2010**, *139*, 154.

15. Maduwage, K.; Isbister, G.K. Current treatment for venom-induced consumption coagulopathy resulting from snakebite. *PLoS Negl. Trop. Dis.* **2014**, *8*, e3220. [CrossRef] [PubMed]

16. Joseph, J.S.; Kini, R.M. Snake venom prothrombin activators homologous to blood coagulation factor Xa. *Pathophysiol. Haemost. Thromb.* **2001**, *31*, 234–240. [CrossRef]

17. Isbister, G.K. (Ed.) Procoagulant snake toxins: Laboratory studies, diagnosis, and understanding snakebite coagulopathy. In *Seminars in Thrombosis Hemostasis*; Thieme Medical Publishers: New York, NY, USA, 2009.

18. Xie, C.; Slagboom, J.; Albulescu, L.O.; Bruyneel, B.; Still, K.; Vonk, F.J.; Somsen, G.W.; Casewell, N.R.; Kool, J. Antivenom neutralization of coagulopathic snake venom toxins assessed by bioactivity profiling using nanofractionation analytics. *Toxins* **2020**, *12*, 53. [CrossRef] [PubMed]

19. Gutiérrez, J.M.; Escalante, T.; Rucavado, A.; Herrera, C. Hemorrhage caused by snake venom metalloproteinases: A journey of discovery and understanding. *Toxins* **2016**, *8*, 93. [CrossRef]

20. Gutiérrez, J.M.; Escalante, T.; Rucavado, A.; Herrera, C.; Fox, J.W. A comprehensive view of the structural and functional alterations of extracellular matrix by snake venom metalloproteinases (SVMPs): Novel perspectives on the pathophysiology of envenoming. *Toxins* **2016**, *8*, 304. [CrossRef]

21. Gutierrez JLeón, G.; Lomonte, B.; Angulo, Y. Antivenoms for snakebite envenomings. *Inflamm. Allergy-Drug Targets* **2011**, *10*, 369–380. [CrossRef]

22. Gutierrez, J.M.; Lomonte, B.; León, G.; Rucavado, A.; Chaves, F.; Angulo, Y. Trends in snakebite envenomation therapy: Scientific, technological and public health considerations. *Curr. Pharm. Des.* **2007**, *13*, 2935–2950. [CrossRef]

23. Lalloo, D.G.; Theakston, R.D.G. Snake antivenoms. *J. Toxicol. Clin. Toxicol.* **2003**, *41*, 277–290. [CrossRef] [PubMed]

24. de Silva, H.A.; Pathmeswaran, A.; Ranasinha, C.D.; Jayamanne, S.; Samarakoon, S.B.; Hittharage, A.; Kalupahana, R.; Ratnatilaka, G.A.; Uluwatthage, W.; Aronson, J.K.; et al. Low-dose adrenaline, promethazine, and hydrocortisone in the prevention of acute adverse reactions to antivenom following snakebite: A randomised, double-blind, placebo-controlled trial. *PLoS Med.* **2011**, *8*, e1000435. [CrossRef] [PubMed]

25. Kularatne, S.A.; Gawarammana, I.B.; Kumarasiri, P.V.; Senanayake, N.; Dissanayake, W.P.; Ariyasena, H. Safety and efficacy of subcutaneous adrenaline as a treatment for anaphylactic reactions to polyvalent antivenom. *Ceylon Med. J.* **2003**, *48*, 148–149. [CrossRef] [PubMed]

26. Casewell, N.R.; Cook, D.A.; Wagstaff, S.C.; Nasidi, A.; Durfa, N.; Wüster, W.; Harrison, R.A. Pre-clinical assays predict pan-African Echis viper efficacy for a species-specific antivenom. *PLoS Negl. Trop. Dis.* **2010**, *4*, e851. [CrossRef] [PubMed]

27. Williams, D.J.; Gutiérrez, J.M.; Calvete, J.J.; Wüster, W.; Ratanabanangkoon, K.; Paiva, O.; Brown, N.I.; Casewell, N.R.; Harrison, R.A.; Rowley, P.D.; et al. Ending the drought: New strategies for improving the flow of affordable, effective antivenoms in Asia and Africa. *J. Proteom.* **2011**, *74*, 1735–1767. [CrossRef]

28. Abubakar, I.S.; Abubakar, S.B.; Habib, A.G.; Nasidi, A.; Durfa, N.; Yusuf, P.O.; Larnyang, S.; Garnvwa, J.; Sokomba, E.; Salako, L.; et al. Randomised controlled double-blind non-inferiority trial of two antivenoms for saw-scaled or carpet viper (Echis ocellatus) envenoming in Nigeria. *PLoS Negl. Trop. Dis.* **2010**, *4*, e767. [CrossRef]

29. Brown, N.I. Consequences of neglect: Analysis of the sub-Saharan African snake antivenom market and the global context. *PLoS Negl. Trop. Dis.* **2012**, *6*, e1670. [CrossRef]

30. Habib, A.G.; Brown, N.I. The snakebite problem and antivenom crisis from a health-economic perspective. *Toxicon* **2018**, *150*, 115–123. [CrossRef]

31. Harrison, R.A.; Hargreaves, A.; Wagstaff, S.C.; Faragher, B.; Lalloo, D.G. Snake envenoming: A disease of poverty. *PLoS Negl. Trop. Dis.* **2009**, *3*, e569. [CrossRef]

32. Laustsen, A.H. Guiding recombinant antivenom development by omics technologies. *New Biotechnol.* **2018**, *45*, 19–27. [CrossRef]

33. Clare, R.H.; Hall, S.R.; Patel, R.N.; Casewell, N.R. Small molecule drug discovery for neglected tropical snakebite. *Trends Pharmacol. Sci.* **2021**, *42*, 340–353. [CrossRef] [PubMed]

34. Albulescu, L.O.; Kazandjian, T.; Slagboom, J.; Bruyneel, B.; Ainsworth, S.; Alsolaiss, J.; Wagstaff, S.C.; Whiteley, G.; Harrison, R.A.; Ulens, C.; et al. A decoy-receptor approach using nicotinic acetylcholine receptor mimics reveals their potential as novel therapeutics against neurotoxic snakebite. *Front. Pharmacol.* **2019**, *10*, 848. [CrossRef]

35. Ye, F.; Zheng, Y.; Wang, X.; Tan, X.; Zhang, T.; Xin, W.; Wang, J.; Huang, Y.; Fan, Q.; Wang, J. Recognition of Bungarus multicinctus venom by a DNA aptamer against β-bungarotoxin. *PLoS ONE* **2014**, *9*, e105404. [CrossRef] [PubMed]

36. Savchik, E.Y.; Kalinina, T.B.; Drozd, N.N.; Makarov, V.A.; Zav'Yalova, E.G.; Lapsheva, E.N.; Mudrik, N.N.; Babij, A.V.; Pavlova, G.V.; Golovin, A.V.; et al. Aptamer RA36 inhibits of human, rabbit, and rat plasma coagulation activated with thrombin or snake venom coagulases. *Bull. Exp. Biol. Med.* **2013**, *156*, 44–48. [CrossRef] [PubMed]

37. Chen, Y.-J.; Tsai, C.-Y.; Hu, W.-P.; Chang, L.-S. DNA aptamers against Taiwan banded krait α-bungarotoxin recognize Taiwan cobra cardiotoxins. *Toxins* **2016**, *8*, 66. [CrossRef] [PubMed]

38. Thiviyanathan, V.; Gorenstein, D.G. Aptamers and the next generation of diagnostic reagents. *PROTEOMICS—Clin. Appl.* **2012**, *6*, 563–573. [CrossRef]

39. Gao, S.; Zheng, X.; Hu, B.; Sun, M.; Wu, J.; Jiao, B.; Wang, L. Enzyme-linked, aptamer-based, competitive biolayer interferometry biosensor for palytoxin. *Biosens. Bioelectron.* **2017**, *89*, 952–958. [CrossRef]

40. Gao, S.; Hu, B.; Zheng, X.; Cao, Y.; Liu, D.; Sun, M.; Jiao, B.; Wang, L. Gonyautoxin 1/4 aptamers with high-affinity and high-specificity: From efficient selection to aptasensor application. *Biosens. Bioelectron.* **2016**, *79*, 938–944. [CrossRef]

41. Marrazza, G. *Aptamer sensors*; Multidisciplinary Digital Publishing Institute: Basel, Switzerland, 2017.

42. Ruscito, A.; DeRosa, M.C. Small-molecule binding aptamers: Selection strategies, characterization, and applications. *Front. Chem.* **2016**, *4*, 14. [CrossRef]

43. Tuerk, C.; Gold, L. Systematic evolution of ligands by exponential enrichment: RNA ligands to bacteriophage T4 DNA polymerase. *Science* **1990**, *249*, 505–510. [CrossRef]

44. Ellington, A.D.; Szostak, J.W. In vitro selection of RNA molecules that bind specific ligands. *Nature* **1990**, *346*, 818–822. [CrossRef] [PubMed]

45. Groff, K.; Brown, J.; Clippinger, A.J. Modern affinity reagents: Recombinant antibodies and aptamers. *Biotechnol. Adv.* **2015**, *33*, 1787–1798. [CrossRef] [PubMed]

46. Nezlin, R. Aptamers in immunological research. *Immunol. Lett.* **2014**, *162*, 252–255. [CrossRef]

47. Ahmadvand, D.; Rahbarizadeh, F.; Moghimi, S.M. Biological targeting and innovative therapeutic interventions with phage-displayed peptides and structured nucleic acids (aptamers). *Curr. Opin. Biotechnol.* **2011**, *22*, 832–838. [CrossRef] [PubMed]

48. Bouchard, P.R.; Hutabarat, R.M.; Thompson, K.M. Discovery and development of therapeutic aptamers. *Annu. Rev. Pharmacol. Toxicol.* **2010**, *50*, 237–257. [CrossRef] [PubMed]

49. Bock, L.C.; Griffin, L.C.; Latham, J.A.; Vermaas, E.H.; Toole, J.J. Selection of single-stranded DNA molecules that bind and inhibit human thrombin. *Nature* **1992**, *355*, 564–566. [CrossRef]

50. Bagheri, E.; Abnous, K.; Alibolandi, M.; Ramezani, M.; Taghdisi, S.M. Triple-helix molecular switch-based aptasensors and DNA sensors. *Biosens. Bioelectron.* **2018**, *111*, 1–9. [CrossRef]

51. Razmi, N.; Baradaran, B.; Hejazi, M.; Hasanzadeh, M.; Mosafer, J.; Mokhtarzadeh, A.; de la Guardia, M. Recent advances on aptamer-based biosensors to detection of platelet-derived growth factor. *Biosens. Bioelectron.* **2018**, *113*, 58–71. [CrossRef]

52. Kim, Y.S.; Raston, N.H.A.; Gu, M.B. Aptamer-based nanobiosensors. *Biosens. Bioelectron.* **2016**, *76*, 2–19.

53. Ronkainen, N.J.; Halsall, H.B.; Heineman, W.R. Electrochemical biosensors. *Chem. Soc. Rev.* **2010**, *39*, 1747–1763. [CrossRef]

54. Chen, A.; Yang, S. Replacing antibodies with aptamers in lateral flow immunoassay. *Biosens. Bioelectron.* **2015**, *71*, 230–242. [CrossRef] [PubMed]

55. Radom, F.; Jurek, P.M.; Mazurek, M.P.; Otlewski, J.; Jeleń, F. Aptamers: Molecules of great potential. *Biotechnol. Adv.* **2013**, *31*, 1260–1274. [CrossRef] [PubMed]

56. Zhu, X.; Yang, J.; Liu, M.; Wu, Y.; Shen, Z.; Li, G. Sensitive detection of human breast cancer cells based on aptamer–cell–aptamer sandwich architecture. *Anal. Chim. Acta* **2013**, *764*, 59–63. [CrossRef] [PubMed]

57. Keefe, A.D.; Pai, S.; Ellington, A. Aptamers as therapeutics. *Nat. Rev. Drug Discov.* **2010**, *9*, 537–550. [CrossRef] [PubMed]

58. Ali, M.H.; Elsherbiny, M.E.; Emara, M. Updates on aptamer research. *Int. J. Mol. Sci.* **2019**, *20*, 2511. [CrossRef]

59. Vater, A.; Klussmann, S. Turning mirror-image oligonucleotides into drugs: The evolution of Spiegelmer® therapeutics. *Drug Discov. Today* **2015**, *20*, 147–155. [CrossRef]

60. Nolte, A.; Klußmann, S.; Bald, R.; Erdmann, V.A.; Fürste, J.P. Mirror-design of L-oligonucleotide ligands binding to L-arginine. *Nat. Biotechnol.* **1996**, *14*, 1116–1119. [CrossRef]

61. Odeh, F.; Nsairat, H.; Alshaer, W.; Ismail, M.A.; Esawi, E.; Qaqish, B.; Bawab, A.A.; Ismail, S.I. Aptamers chemistry: Chemical modifications and conjugation strategies. *Molecules* **2019**, *25*, 3. [CrossRef]

62. Sundaram, P.; Kurniawan, H.; Byrne, M.E.; Wower, J. Therapeutic RNA aptamers in clinical trials. *Eur. J. Pharm. Sci.* **2013**, *48*, 259–271. [CrossRef]

63. Bunka, D.H.J.; Platonova, O.; Stockley, P.G. Development of aptamer therapeutics. *Curr. Opin. Pharmacol.* **2010**, *10*, 557–562. [CrossRef]

64. Toh, S.Y.; Citartan, M.; Gopinath, S.C.B.; Tang, T.-H. Aptamers as a replacement for antibodies in enzyme-linked immunosorbent assay. *Biosens. Bioelectron.* **2015**, *64*, 392–403. [CrossRef] [PubMed]

65. Ni, S.; Yao, H.; Wang, L.; Lu, J.; Jiang, F.; Lu, A.; Zhang, G. Chemical modifications of nucleic acid aptamers for therapeutic purposes. *Int. J. Mol. Sci.* **2017**, *18*, 1683. [CrossRef] [PubMed]

66. Kong, H.Y.; Byun, J. Nucleic acid aptamers: New methods for selection, stabilization, and application in biomedical science. *Biomol. Therapeut.* **2013**, *21*, 423. [CrossRef] [PubMed]

67. Fischer, M.J.M.; Schmidt, J.; Koulchitsky, S.; Klussmann, S.; Vater, A.; Messlinger, K. Effect of a calcitonin gene-related peptide-binding L-RNA aptamer on neuronal activity in the rat spinal trigeminal nucleus. *J. Headache Pain* **2018**, *19*, 3. [CrossRef] [PubMed]

68. Bruno, J.G.; Carrillo, M.P.; Phillips, T.; Vail, N.K.; Hanson, D. Competitive FRET-aptamer-based detection of methylphosphonic acid, a common nerve agent metabolite. *J. Fluoresc.* **2008**, *18*, 867–876. [CrossRef]

69. Sun, W.; Du, L.; Li, M. Aptamer-based carbohydrate recognition. *Curr. Pharm. Des.* **2010**, *16*, 2269–2278. [CrossRef]

70. Ma, L.-H.; Wang, H.-B.; Fang, B.-Y.; Tan, F.; Cao, Y.-C.; Zhao, Y.-D. Visual detection of trace lead ion based on aptamer and silver staining nano-metal composite. *Colloids Surf. B Biointerfaces* **2018**, *162*, 415–419. [CrossRef]

71. Emahi, I.; Gruenke, P.R.; Baum, D.A. Effect of aptamer binding on the electron-transfer properties of redox cofactors. *J. Mol. Evol.* **2015**, *81*, 186–193. [CrossRef]

72. Chabata, C.V.; Frederiksen, J.W.; Sullenger, B.A.; Gunaratne, R. Emerging applications of aptamers for anticoagulation and hemostasis. *Curr. Opin. Hematol.* **2018**, *25*, 382–388. [CrossRef]

73. Song, K.-M.; Lee, S.; Ban, C. Aptamers and their biological applications. *Sensors* **2012**, *12*, 612–631. [CrossRef]

74. Lauridsen, L.H.; Shamaileh, H.A.; Edwards, S.L.; Taran, E.; Veedu, R.N. Rapid one-step selection method for generating nucleic acid aptamers: Development of a DNA aptamer against α-bungarotoxin. *PLoS ONE* **2012**, *7*, e41702. [CrossRef] [PubMed]

75. Anand, A.; Chatterjee, B.; Dhiman, A.; Goel, R.; Khan, E.; Malhotra, A.; Santra, V.; Salvi, N.; Khadilkar, M.V.; Bhatnagar, I.; et al. Complex target SELEX-based identification of DNA aptamers against Bungarus caeruleus venom for the detection of envenomation using a paper-based device. *Biosens. Bioelectron.* **2021**, *193*, 113523. [CrossRef] [PubMed]

76. Alomran, N.; Blundell, P.; Alsolaiss, J.; Crittenden, E.; Ainsworth, S.; Dawson, C.A.; Edge, R.J.; Hall, S.R.; Harrison, R.A.; Wilkinson, M.C.; et al. Exploring the utility of recombinant snake venom serine protease toxins as immunogens for generating experimental snakebite antivenoms. *Toxins* **2022**, *14*, 443. [CrossRef]

77. Alomran, N.; Alsolaiss, J.; Albulescu, L.O.; Crittenden, E.; Harrison, R.A.; Ainsworth, S.; Casewell, N.R. Pathology-specific experimental antivenoms for haemotoxic snakebite: The impact of immunogen diversity on the in vitro cross-reactivity and in vivo neutralisation of geographically diverse snake venoms. *PLoS Negl. Trop. Dis.* **2021**, *15*, e0009659. [CrossRef]

78. Castro, H.C.; Zingali, R.B.; Albuquerque, M.G.; Pujol-Luz, M.; Rodrigues, C.R. Snake venom thrombin-like enzymes: From reptilase to now. *Cell. Mol. Life Sci. CMLS* **2004**, *61*, 843–856. [CrossRef]

79. Serrano, S.M.T.; Maroun, R.C. Snake venom serine proteinases: Sequence homology vs. substrate specificity, a paradox to be solved. *Toxicon* **2005**, *45*, 1115–1132. [CrossRef] [PubMed]

80. Clauss, A. Gennungsphysiologishe schnellmethode sur Bestimmung des Fibrinogens. *Acta Haematol.* **1957**, *17*, 237–246. [CrossRef]

81. Knudsen, C.; Ledsgaard, L.; Dehli, R.I.; Ahmadi, S.; Sørensen, C.V.; Laustsen, A.H. Engineering and design considerations for next-generation snakebite antivenoms. *Toxicon* **2019**, *167*, 67–75. [CrossRef] [PubMed]

82. Zhang, W.; Liu, Q.X.; Guo, Z.H.; Lin, J.S. Practical application of aptamer-based biosensors in detection of low molecular weight pollutants in water sources. *Molecules* **2018**, *23*, 344. [CrossRef] [PubMed]

83. Eissa, S.; Ng, A.; Siaj, M.; Tavares, A.C.; Zourob, M. Selection and identification of DNA aptamers against okadaic acid for biosensing application. *Anal. Chem.* **2013**, *85*, 11794–11801. [CrossRef]

84. Eissa, S.; Ng, A.; Siaj, M.; Zourob, M. Label-free voltammetric aptasensor for the sensitive detection of microcystin-LR using graphene-modified electrodes. *Anal. Chem.* **2014**, *86*, 7551–7557. [CrossRef] [PubMed]

85. Eissa, S.; Siaj, M.; Zourob, M. Aptamer-based competitive electrochemical biosensor for brevetoxin-2. *Biosens. Bioelectron.* **2015**, *69*, 148–154. [CrossRef] [PubMed]

86. El-Aziz, T.M.; Ravelet, C.; Molgo, J.; Fiore, E.; Pale, S.; Amar, M.; Al-Khoury, S.; Dejeu, J.; Fadl, M.; Ronjat, M.; et al. Efficient functional neutralization of lethal peptide toxins in vivo by oligonucleotides. *Sci. Rep.* **2017**, *7*, 7202. [CrossRef]

87. Kini, R.M. Serine proteases affecting blood coagulation and fibrinolysis from snake venoms. *Pathophysiol. Haemost. Thrombos.* **2005**, *34*, 200–204. [CrossRef] [PubMed]

88. Brody, E.N.; Gold, L. Aptamers as therapeutic and diagnostic agents. *Rev. Mol. Biotechnol.* **2000**, *74*, 5–13. [CrossRef]

89. Ravelet, C.; Grosset, C.; Peyrin, E. Liquid chromatography, electrochromatography and capillary electrophoresis applications of DNA and RNA aptamers. *J. Chromatogr. A* **2006**, *1117*, 1–10. [CrossRef]

90. Cao, Z.; Tan, W. Molecular Aptamers for Real-Time Protein-Protein Interaction Study. *Chem. Eur. J.* **2005**, *11*, 4502–4508. [CrossRef]

91. Chen, Z.; Ruffner, D.E. Modified crush-and-soak method for recovering oligodeoxynucleotides from polyacrylamide gel. *Biotechniques* **1996**, *21*, 820–822. [CrossRef]

92. Simossis, V.A.; Heringa, J. The PRALINE online server: Optimising progressive multiple alignment on the web. *Comput. Biol. Chem.* **2003**, *27*, 511–519. [CrossRef]